Gamma Rays from Neutron Inelastic Scattering*

ROBERT B. DAY
Los Alamos Scientific Laboratory, Los Alamos, New Mexico
(Received January 30, 1956)

A NaI scintillation counter has been used to observe gamma rays from neutron inelastic scattering in B^{10}, C, N, O, F, Mg, Al, S, Ca, Fe, Ni, Cu, Ta, Pb, and Bi. In most cases these gamma rays can be fitted into known level schemes of the target nuclides; however, a few gamma rays require the existence of previously undetected levels. In addition, several gamma rays have been observed from $(n,p'\gamma)$ and $(n,\alpha'\gamma)$ reactions. The problems involved in measuring absolute cross sections for the production of gamma rays are considered in detail. The usefulness of neutron inelastic scattering in nuclear spectroscopy is illustrated in several cases.

I. INTRODUCTION

THE inelastic scattering of neutrons by nuclei has presented an important problem for many years, not only because of its influence on the passage of neutrons through matter but also because the results of such measurements can be used to gain information on the level structure of nuclei and to test various nuclear models. Despite the importance of such measurements, it has only been in recent years that experimental techniques have been developed to the point that accurate cross sections can be measured and the spectra of the inelastically scattered neutrons determined.

There are several reasons for this delay. One is that for many years it was difficult to obtain a satisfactory source of monoenergetic neutrons. With the development of electrostatic accelerators and the availability of deuterium and tritium, one can now use the $H^3(p,n)He^3$, $H^2(d,n)He^3$, and $H^3(d,n)He^4$ reactions as variable energy sources of monoenergetic neutrons with sufficient intensity for many inelastic scattering experiments. The $Li^7(p,n)Be^7$ reaction is often used also, but the presence of two neutron groups here is sometimes a disadvantage.

A second difficulty is the problem of obtaining a detector with sufficiently good resolution to separate the various groups of inelastically scattered neutrons. Photographic emulsions have provided a means of measuring neutron spectra, but the tedious process of measuring and counting the proton recoil tracks has inhibited the widespread use of this technique. Counter techniques based on the measurement of proton recoil energies have also been developed for the measurement of neutron energies. These generally fall into one of two classes: (1) counters with an output that gives the differential spectrum as a function of energy, and (2) counters that give an integral spectrum. The first class usually has a very low detection efficiency. Although the second can have high efficiency, this is offset by the fact that the output spectrum must be differentiated in order to deduce the neutron spectrum. Because of these deficiencies, proton recoil counter techniques have found only a very limited application in neutron inelastic scattering measurements. The development in the past year of fast neutron time-of-flight techniques,[1] however, has provided a method of measuring fast neutron spectra that has fairly good resolution and reasonable efficiency.

Because of the difficulties involved in measuring neutron spectra at the time this work was begun, it seemed advantageous to attempt to make measurements of neutron inelastic scattering from a different point of view. In most cases a nucleus that is raised to an excited state will decay to its ground state with the emission of gamma radiation. Since methods of gamma-ray spectroscopy have already been developed, these can readily be adapted to the problem of detecting the gamma rays accompanying inelastic scattering. In particular the NaI scintillation spectrometer combines fair resolution with good detection efficiency and has, therefore, proved to be a most useful tool in these studies.

For levels that are high enough to be unstable to particle emission this method is of little value since the relative probability of gamma-ray emission is generally so low that the gamma rays will not be detected above the background. Although there are examples of unbound levels where particle emission is forbidden, these are few. An additional difficulty occurs for levels that are highly internally converted. Since the internal conversion electrons are largely absorbed in the neutron scatterer, transitions of this type are difficult to detect. These considerations indicate that the usefulness of gamma-ray spectra in measurements of neutron inelastic scattering will be greatest in the lighter elements and for incident neutron energies below the neutron binding energy of the target nucleus. There are, however, many examples among the heavy nuclei where this technique is still useful since the internal conversion is often not too large except for low-energy or high multipole-order transitions.

In a number of recent experiments[2] the techniques of

* Work performed under the auspices of the U. S. Atomic Energy Commission.

[1] L. Cranberg, International Conference on the Peaceful Uses of Atomic Energy, Geneva, 1955 (to be published). L. Cranberg and J. S. Levin, Phys. Rev. **100**, 434 (1955).

[2] Scherrer, Theus, and Faust, Phys. Rev. **89**, 1268 (1953); **91**, 1476 (1953); Scherrer, Smith, Allison, and Faust, Phys. Rev. **91**,

gamma-ray spectroscopy have been applied to the problem of neutron inelastic scattering. In the following sections are presented the results of experiments on the gamma rays following neutron inelastic scattering[3] together with a discussion of the techniques used to obtain accurate cross sections for these reactions. In a number of cases the usefulness of neutron inelastic scattering in determining energy levels and decay schemes is also illustrated.

II. EXPERIMENTAL PROCEDURE

The counter used for gamma-ray detection consisted of a sodium iodide crystal 2.57 cm long and 2.54 cm in diameter mounted on a DuMont 6292 photomultiplier. The crystal was hermetically sealed in an aluminum container with walls 0.4 mm thick and was attached to the photomultiplier by a thin aluminum collar held in place by black electrical tape. The resolution of this detector for the Cs^{137} 662-kev gamma ray was 8%.

Pulses from the scintillation counter were amplified in a Los Alamos Model 250 amplifier and preamplifier.[4] This is a nonoverloading amplifier having very good linearity and stability. After amplification the pulses were analyzed in a 10-channel pulse-height analyzer designed by Johnstone.[5] For some of the later work a much-improved version of the Hutchinson-Scarrott 100-channel analyzer was used.[6] Since this analyzer had an average dead time of 500 μsec, it was necessary to run a fast single-channel analyzer in parallel with it in order to make a correction for counting losses.

Monoenergetic neutrons were produced by the $H^3(p,n)He^3$ reaction by bombarding a tritium gas cell with protons from the large Los Alamos electrostatic accelerator. The protons were analyzed by a magnet with a momentum resolution of about 0.1%. The main contributions to the spread in neutron energy arose from the stopping power of the tritium gas and from nonuniformities in the 0.0012-mm nickel foil at the entrance to the gas target. For most of the measurements reported here the average neutron energy at the scatterer was 2.557 ± 0.010 Mev, and the spread in energy (full width at half-maximum) was about 30 kev. The spread in energy was measured by observing the width of the transmission dip at the 2.087-Mev resonance in carbon and extrapolating to the higher energy. The position of this resonance also gave a check on the calculated neutron energy. For a number of elements where the first level could not be excited by 2.56-Mev neutrons, higher energies were used. Neutrons above 4 Mev in energy were produced by the $H^2(d,n)He^3$ reaction. Except for the change in the neutron source reaction, conditions were the same. The neutron source strength was monitored by a "long counter"[7] placed 160 cm from the target at 90° to the beam.

The experimental arrangement used in these experiments is shown in Fig. 1. The scintillation counter was mounted on the axis of the proton beam 40 cm from the center of the gas target. Shielding it from the direct neutron beam was a tungsten alloy cone 30 cm long. The diameters of the cone at the small and large ends were 0.64 cm and 3.02 cm, respectively. Scattering rings of various elements were suspended symmetrically about the crystal with their axes along the crystal axis. These rings had an inside diameter of 5.08 cm and an outside diameter of 7.08 cm or 10.16 cm. The smaller rings were used with the denser materials in order to reduce self-absorption of the gamma rays. The axial thickness of the rings was generally adjusted to give a neutron transmission of about 0.75, although for a number of elements rings of about twice this thickness were also used in investigating the effects of neutron multiple scattering. The shielding cone and scattering rings were suspended by light wires or strings, and in general all extraneous scattering material was kept at a distance.

In measuring gamma-ray energies the effects of nonlinearities and slow drifts in gain of the electronic equipment were eliminated with the aid of a precision pulse generator. Pulses from this could be fed into the preamplifier in parallel with the photomultiplier and adjusted to give pulses at the amplifier output of the same size as those occurring at peaks in the pulse-height distribution being analyzed. The calibration of pulse height in terms of gamma-ray energy was made by measuring the pulse heights of a number of gamma rays of known energy. Above 400 kev the pulse height was linear with energy within $\frac{1}{3}$%; however, at lower energies a nonlinearity occurred in the scintillation counter that made the measurement of gamma-ray energies less accurate, except in the energy regions near calibration points. In order to minimize errors due to gain shifts in the photomultiplier with counting rate,[8] the counting rate was generally kept an order of magnitude lower than that at which shifts of several percent were noticeable. In addition the energy calibrations

768 (1953); Scherrer, Allison, and Faust, Phys. Rev. **96**, 386 (1954); R. M. Kiehn and C. Goodman, Phys. Rev. **93**, 177 (1954); **95**, 989 (1954); Eliot, Hicks, Beghian, and Halban, Phys. Rev. **94**, 144 (1954); L. C. Thomson and J. R. Risser, Phys. Rev. **94**, 941 (1954); M. A. Rothman and C. E. Mandeville, Phys. Rev. **93**, 796 (1954); Rothman, Hans, and Mandeville, Phys. Rev. **100**, 83 (1955); Rayburn, Lafferty, and Hahn, Phys. Rev. **94**, 1641 (1954); **96**, 381 (1955); **98**, 701 (1955); G. L. Griffith, Phys. Rev. **98**, 579 (1955); R. M. Sinclair, Phys. Rev. **99**, 1351 (1955); Garrett, Hereford, and Sloope, Phys. Rev. **92**, 1507 (1953); M. E. Battat and E. R. Graves, Phys. Rev. **97**, 1266 (1955); Freeman, Lane, and Rose, Phil. Mag. **46**, 17 (1955); J. M. Freeman, Phil. Mag. **46**, 12 (1955); Phys. Rev. **99**, 1446 (1955); Beghian, Hicks, and Milman, Phil. Mag. **46**, 924, 963 (1955); J. J. Van Loef, thesis, Utrecht, 1955 (unpublished).

[3] A preliminary report on part of this work has been given [R. B. Day, Phys. Rev. **89**, 908(A) (1953)].

[4] C. W. Johnstone, Los Alamos Scientific Laboratory Report LA-1878 (unpublished).

[5] C. W. Johnstone, Nucleonics **11**, No. 1, 36 (1953).

[6] J. D. Gallagher, Los Alamos Scientific Laboratory Report LA-1917 (unpublished); McKibben, Gallagher, and Lang, Inst. Radio Engrs., Convention Record **3**, Part 10, 186 (1955).

[7] A. O. Hanson and J. L. McKibben, Phys. Rev. **72**, 673 (1947).

[8] Bell, Davis, and Bernstein, Rev. Sci. Instr. **26**, 726 (1955).

with standard sources were made at about the same counting rates as those obtained from the inelastic scattering experiments so that any small gain shifts would tend to be canceled out.

III. CROSS-SECTION MEASUREMENTS

To obtain the cross sections for gamma-ray production by neutron inelastic scattering, one must know both the gamma-ray yield and the neutron flux incident on the scatterer, as well as the number of nuclei in the scatterer. These points are considered in detail in the following sections.

1. Gamma-Ray Yield

Because of the complexity of the pulse-height spectra produced in the scintillation counter, one can generally use only the photopeaks in determining the gamma-ray yields. To convert the number of counts in the photopeak to a gamma-ray yield, it is necessary to know the photopeak efficiency for the geometrical arrangement of source and detector used. Calculations of the photopeak efficiency have been reported,[9,10] but these have applied only to point sources with the radiation incident on the flat face of a cylindrical crystal. Because of the complication of extending such calculations to the case of an extended ring source surrounding a cylindrical crystal, it seemed preferable to determine the photopeak efficiency empirically.

The method used was to measure the number of counts produced in the photopeak by calibrated gamma-ray sources. The sources were solutions of Au^{198}(0.412 Mev), Na^{22}(0.511 and 1.277 Mev), Nb^{95}(0.764 Mev), Sc^{46}(0.885 and 1.119 Mev), and Na^{24}(1.370 and 2.754 Mev) in thin-wall toroidal containers having the same dimensions as the scattering rings, namely (1) i.d.=5.08 cm, o.d.=10.16 cm, thickness=1.27 cm, and (2) i.d. =5.08 cm, o.d.=7.08 cm, thickness=1.00 cm. The containers were machined of polyethylene in order to reduce gamma-ray absorption and to avoid plating of the radioactive material on the walls. With these sources the actual geometrical conditions occurring in the scattering experiments could be duplicated. The variation of the photopeak efficiency as a function of the axial position of the source was also measured in order to correct for the different thicknesses of the scatterers that were used. In the neutron experiments the scattering ring could be placed symmetrically about the scintillation crystal to an accuracy of better than 1 mm. To test the effect of possible positioning errors, the sources were displaced axially and radially about 1 mm. Since there was no detectable change in the counting rate it was concluded that no appreciable error could arise in this way.

The determination of the gamma-ray intensity of the sources was carried out by the β-γ coincidence method.[11] Both the β and γ detectors were scintillation counters, the β counter generally having a 0.7-mm thick anthracene crystal and the γ counter a large NaI(Tl) crystal. Since the principal uncertainty in measurements of this kind arises from the sensitivity of the β counter to gamma rays, particular care was taken in determining this quantity. It was possible to calculate this sensitivity, and these calculations were in agreement with the experimentally determined values. In most cases the correction to the gamma-ray source strength for this effect was only of the order of 1%. Corrections for background and for accidental coincidences were kept small and were generally of the order of 1 to 3%. The sources were very thin to β particles and were placed far enough from the β detector so that its efficiency was approximately constant over the entire source. To check on the possibility of errors from coincidence losses due to rise-time delays and from possible after-pulses in the photomultiplier, the operating conditions of the detectors and their associated equipment were varied over a wide range. The gamma-ray source strength was independent of these parameters in all cases, as was to be expected.

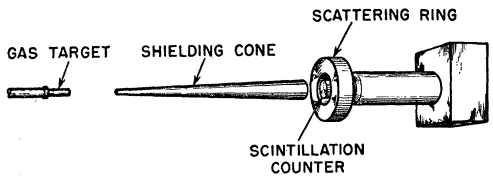

FIG. 1. Experimental arrangement for measuring gamma rays from neutron inelastic scattering.

The Na^{22}, Nb^{95}, and Sc^{46} were obtained from Oak Ridge and were stated to have a radioactive purity of >99%, except for Nb^{95}, which was >98%. The Au^{198} and Na^{24} were prepared by neutron activation in the Los Alamos Water Boiler reactor. In the case of Au^{198}, care was taken to keep the neutron flux low enough to avoid the formation of an appreciable amount of Au^{199}. Preliminary experiments showed that the half-lives of Au^{198} and Na^{24} thus prepared agreed within 1 percent with the best values in the literature[12]; furthermore, this was confirmed by the agreement of the β-γ coincidence measurements after correction for decay. Standard solutions of these high-purity sources were prepared, from which accurately measured aliquots were withdrawn and evaporated to dryness. At least three of these were counted for each solution to be standardized. The standard deviation of these source strength determinations, as determined from their internal consistency, was generally less than 1%.

[9] Maeder, Müller, and Wintersteiger, Helv. Phys. Acta **27**, 3 (1954).
[10] M. J. Berger and J. A. Doggett, Phys. Rev. **99**, 663 (1955).
[11] J. L. Putman, Brit. J. Radiol. **23**, 46 (1950).
[12] Hollander, Perlman, and Seaborg, Revs. Modern Phys. **25**, 469 (1953); P. M. Endt and J. C. Kluyver, Revs. Modern Phys. **26**, 95 (1954); E. E. Lockett and R. H. Thomas, Nucleonics **11**, No. 3, 14 (1953); R. E. Bell and L. Yaffe, Can. J. Phys. **32**, 416 (1954).

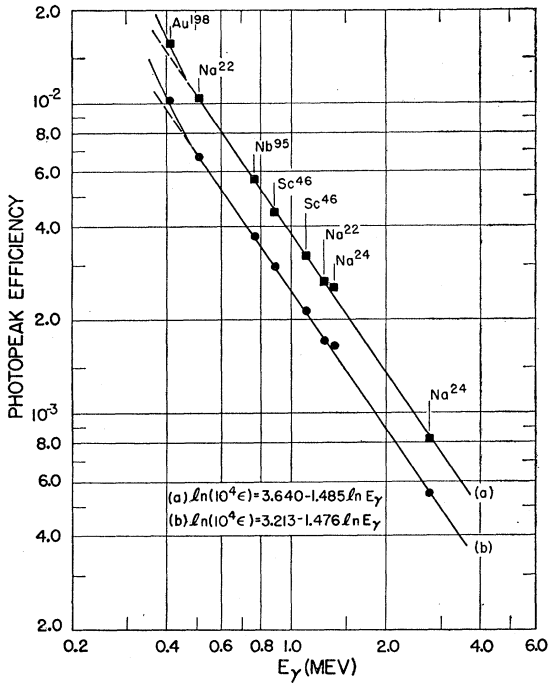

FIG. 2. Photopeak efficiency of a NaI crystal 2.57 cm long and 2.54 cm in diameter for ring sources placed symmetrically about the crystal as in Fig. 1. The sources were enclosed in toroids of rectangular cross section with the following dimensions: (a) o.d. = 7.08 cm, i.d. = 5.08 cm, thickness = 1.00 cm; (b) o.d. = 10.16 cm, i.d. = 5.08 cm, thickness = 1.27 cm. The curves are corrected for self-absorption in the sources.

After the solution had been standardized, an aliquot of suitable strength was withdrawn and placed in one of the polyethylene toroids. Water was then added to fill the entire volume of the toroid. This was suspended symmetrically about the NaI crystal whose efficiency was to be determined, and the photopeak counting rate was measured. The photopeak efficiency could then be obtained after small corrections had been made for gamma-ray absorption in the source and coincident detection of gamma rays in the three cases where more than one gamma ray is emitted. These corrections were calculated in a manner to be described later in this section. The results of the measurements of the photopeak efficiency for a crystal 2.57 cm long and 2.54 cm in diameter are given as a function of gamma-ray energy in Fig. 2. For both source geometries it is seen that the logarithm of the photopeak efficiency is a linear function of the logarithm of the gamma-ray energy for energies between 0.5 and 2.8 Mev. The rms deviation of the experimental points from a linear least-squares fit in this region is 1.8% for the larger toroid and 2.6% for the smaller. The reason for the large deviation of the point at 1.37 Mev (Na^{24}) is not understood. If one eliminates this point, the root-mean-square deviation of the other experimental points between 0.5 and 2.8 Mev from a linear least-squares fit is reduced to 1.0% in both cases. From these results it appears that the photopeak efficiency is known between 0.5 and 2.8 Mev to an accuracy of about 2%. Between 0.4 and 0.5 Mev the efficiency deviates from this simple power law, and the accuracy is correspondingly reduced.

At gamma-ray energies below 0.4 Mev and above 2.8 Mev, it was not possible to obtain radionuclides whose decay schemes were known as well as those used above. At these higher and lower energies, the procedure used was to calculate the total efficiency for producing a pulse in the NaI crystal and to multiply this efficiency by the ratio of the number of pulses in the photopeak to the total number of pulses produced by the gamma ray. (Above 3 Mev the pair peak was used instead of the photopeak.) This ratio was obtained experimentally at a number of different gamma-ray energies and a smooth curve was drawn through the points. The theoretical results of Maeder *et al.*[9] and of Berger and Doggett[10] were used as an aid in getting the correct shape of this curve.

If one has a plane wave of neutrons parallel to the z_1-axis of a scattering ring, the number of pulses produced in the gamma-ray detector is proportional to the quantity

$$P=\frac{1}{4\pi V_1}\int\int\frac{e^{-\mu z_1}e^{-\mu_1 l_1}e^{-\mu_2 l_2}}{r_{12}^2}\mu_2 dV_2 dV_1, \qquad (1)$$

where μ is the neutron attenuation coefficient in the ring, μ_1 is the gamma-ray absorption coefficient in the ring, l_1 is the path length of the gamma ray in the ring, μ_2 and l_2 are the corresponding quantities in the detector, r_{12} the distance between volume elements in the ring and detector, and V_1 and V_2 refer to the volumes of the ring and detector. Because of the nature of the expression for l_1, l_2, and r_{12}, this integral cannot be integrated in closed form. Accordingly, a numerical evaluation by means of Simpson's rule was carried out on a high-speed digital computer (the Los Alamos MANIAC). The quantity μ_2 is the absorption coefficient in NaI and is proportional to the sum of the cross sections for the photoelectric effect, Compton scattering, and pair production. The appropriate cross sections were obtained from the compilation of White.[13]

The factor $e^{-\mu z_1}$ was included here only to approximate the source distribution of gamma rays in the scattering ring. Calculations showed that for the scattering rings used in these experiments, the NaI counter efficiency was essentially independent of whether the gamma rays had an exponential or uniform distribution in the ring. Furthermore, the effects of multiple neutron scattering tended to make the distribution more uniform. Therefore, this exponential could have been omitted from the efficiency and self-absorption calculations.

The total efficiency of the detector can be obtained

[13] G. R. White, National Bureau of Standards Report NBS-1003, 1952 (unpublished).

by evaluating the expression for P with $\mu=0$. These values were compared with experimental values for the total efficiency that were obtained with the calibrated gamma-ray sources. The agreement between these two ways of determining the total efficiency was within the experimental accuracy of 5 to 10%.

Since the scattering samples did not all have the same axial thickness, it was necessary to make a correction for the variation of efficiency with length. This correction was obtained experimentally from a determination of the photopeak efficiency as a function of the axial position of several toroidal gamma-ray sources, and also by calculation from the expression for P. Since the experimental and calculated values were in good agreement, the calculated corrections were used thereafter. The maximum correction required was only 5%.

In order to obtain the true gamma-ray yield from a scattering ring, it is necessary to correct for self-absorption in the ring. This correction was obtained from the ratio $P(\mu_1=0)/P(\mu_1)$. A difficulty here lies in determining what to use for μ_1, since the entire Compton scattering cross section does not contribute to the gamma-ray absorption. The effective absorption coefficients for Al and Fe at six energies between 0.1 Mev and 2.8 Mev were obtained from gamma-ray transmission experiments in a geometry close to that used in the neutron inelastic scattering experiments; i.e., the gamma-ray sources were placed on top of the absorbers and at a distance from the center of the NaI crystal equal to the average radius of the scattering rings. The effective absorption cross sections were also calculated in the following way. Compton scattering interactions were considered as inelastic gamma-ray scattering in which the direction of the gamma ray was unchanged. Thus the gamma ray is effectively absorbed only if its energy is reduced sufficiently to place it below the energy band included in the photopeak of the NaI detector. Knowing the photopeak width, one can then calculate an effective Compton cross section. The total cross section was obtained by adding this to the photoelectric and pair cross sections obtained from the tables calculated by White.[13] The cross sections calculated in this way agreed within 2% with the cross sections obtained from the transmission measurements, except at gamma-ray energies below 200 kev. The cross sections used in the integral for P were obtained in this manner, but with the photopeak width adjusted slightly to give better agreement with the experimentally determined cross sections. At energies below 200 kev the absorption coefficients were obtained experimentally.

2. Neutron Flux Measurements

During the course of the inelastic scattering measurements, the neutron flux was monitored by a long counter placed at 90° to the beam. In order to obtain the neutron flux incident on the ring scatterer in terms of the monitor count, the shielding cone, ring, and detector were removed, and a second long counter was placed at 0° to the beam, subtending the same angle as the scattering ring. The ratio of the counting rates in the two long counters was then measured for each neutron energy, and the absolute efficiency of the second long counter was obtained with the aid of a Ra-Be source placed at the position of the center of the target. The statistical accuracy of such calibrations was 1% or better; however, in a number of determinations of the constant relating the monitor counting rate to the neutron flux at the scatterer, the standard deviation of these measurements was 1.8%. This higher figure presumably reflects the effect of possible shifts in the amplifier gain and bias setting over a period of several weeks. The usual background corrections were obtained by measuring the counting rates with the long counters shielded by a large paraffin cone and also with the target cell evacuated. However, no correction for room-scattered neutrons was applied to the monitor at 90°, since this is a constant effect that is proportional to the total flux.

A number of corrections have to be applied to the flux calibration constant mentioned above. In the first place, it is known that many Ra-Be sources do not have an isotropic intensity distribution. For this reason, the angular distribution of neutrons from the standard source was measured with a long counter and a small correction was applied for its anisotropy. By proper orientation of the source this correction could be made less than 1%. Second, a correction for counting losses in the long counters had to be applied, which was generally less than 2%. This correction was obtained experimentally by the two-source method and by measuring the total number of neutron counts for a fixed charge as the proton beam current was varied. The two methods gave results in general agreement although the second cannot be considered as reliable as the first because of local heating of the tritium gas by the beam, which causes a reduction in neutron yield.

Third, one must consider the possible difference in long-counter efficiency for a Ra-Be source and for monoenergetic neutrons of the energies used here. Measurements have shown that the long-counter efficiency is constant within 2% for various polyenergetic sources, but that at neutron scattering resonances in carbon it exhibits variations of the order of 5%.[14] Since none of the work reported here was done at neutron energies near carbon resonances, this latter effect could be neglected. However, recent investigations of the long-counter efficiency for monoenergetic neutrons have shown that the efficiency is not flat at all but has slow variations of as much as 15%.[15] These results were obtained by comparing the counting

[14] Nobles, Day, Henkel, Jarvis, Kutarnia, McKibben, Perry, and Smith, Rev. Sci. Instr. **25**, 334 (1954).

[15] J. E. Perry, Jr. (private communication). I am indebted to Dr. Perry for permission to use these results before publication.

rate in the long counter with that in a "counter telescope" which counted the proton recoils from a polyethylene radiator that were emitted into a fixed solid angle. The counter telescope gives absolute neutron fluxes with a standard error of 3% or less. The efficiency of the long counter as determined in this manner is 6% higher at 2.56 Mev than the efficiency obtained using a calibrated Ra-Be source and assuming the long-counter efficiency to be constant.[16] The corrections obtained from Perry's work were used here; however, because of the apparent discrepancy with the earlier work of Nobles *et al.*, the standard error in the neutron flux was doubled and taken to be 6%. The neutron flux calibration is independent of the absolute value of the Ra-Be source since the source is now used only to provide a reference flux.

The effect of the tungsten cone on the neutron flux at the scattering ring was investigated by removing the ring and placing a stilbene scintillation counter at the same position. The pulse-height spectrum from this counter was then observed with the cone in place and with it removed. There was no detectable change in the shape of the pulse-height distribution; furthermore, the integral number of counts under the pulse-height distribution was the same within 1%. Thus the cone has no effect on the fast neutron flux.

The possible presence of thermal neutrons was tested by placing a U^{235} fission ionization chamber at the ring position, leaving the cone in place. The difference in the counting rates of this chamber with and without a cadmium cover is then a measure of the thermal neutron contamination. Since the counting rates were the same within the statistical error of 3%, it is apparent that the thermal neutron contamination was negligible.

A test for epithermal neutrons was made by measuring the counting rate in a BF_3 proportional counter when it was shielded from the neutron source by the tungsten cone. This counting rate was of the order of one-half the counting rate with the cone removed. Since the relative background of a fast-neutron counter, such as a long counter, as measured in this way is only about 2%, it appears that there is a small number of epithermal neutrons present. Thus reactions that have a large cross section in this region, such as $B^{10}(n,\alpha)Li^7$, cannot easily be measured with accuracy.

It is generally assumed that the $T(p,n)$ and $D(d,n)$ reactions give monoenergetic neutrons for bombarding energies below 4.4 Mev. However, this assumption neglects the possibility that unforeseen experimental difficulties can affect the spectrum. Over the past few years a number of measurements have been made by L. Rosen of the neutron spectra produced by these reactions.[17] The results after subtraction of all backgrounds indicate that a small fraction of the total number of neutrons (of the order of 2 to 3%) may have energies below that calculated. The origin of these lower energy neutrons is not understood. It is clear, however, that their possible presence must be considered in accurate neutron experiments.

Closely allied with the problem of neutron flux measurement is that of neutron multiple scattering in the scatterer. Ordinarily one assumes that each neutron interacts only once in the scatterer, which leads to the usual exponential neutron flux distribution. However, after being scattered once, there is often a good chance that a neutron will be scattered again. The probability for this depends on the dimensions of the scatterer and the scattering cross sections. If one assumes that a plane wave of neutrons is normally incident on the scatterer along the z-axis, the gamma-ray yields resulting from the first and second scatterings can be written

$$Y_1 = N_0(1-e^{-\mu d})\frac{\sigma_{in}}{\sigma_t}, \tag{2}$$

$$Y_2 = \frac{\sigma_{in}}{\sigma_t}k_2\frac{N_0 d}{V}\int\int e^{-\mu z}n\frac{d\sigma(\theta)}{d\Omega}(1-e^{-\mu l})dV d\Omega, \tag{3}$$

where N_0 is the number of neutrons incident on the scatterer, σ_t and σ_{in} are the total and inelastic scattering cross sections, μ the total attenuation coefficient, d the scatterer thickness, n the number of nuclei per cm^3, $d\sigma(\theta)/d\Omega$ the differential scattering cross section, l the neutron path length to the surface of the ring after the first scattering, and k_2 the fraction of neutrons that can produce an inelastic event after their first interaction.

It was clear from early experiments that Eq. (2) was not satisfactory since cross sections calculated using it alone did not agree when different sizes of scatterers were used for the same element. Therefore, Eq. (3) was also included in the cross-section calculations to take multiple scattering into account. The integral was evaluated numerically on a high-speed computer by using the Gauss integration formula. At the time these calculations were originally made, the only angular distributions that had been measured for neutrons in the energy range of interest were those of Jurney and Zabel[18] using a beam of fission spectrum neutrons and U^{238} or Np^{237} fission ionization chambers as detectors. The median neutron energies for fission spectrum neutrons measured with these detectors are 2.5 Mev and 1.0 Mev, respectively, while the average energies are 3.0 Mev and 2.5 Mev. Thus the angular distributions measured with the U^{238} detector should be representative of the true angular distributions for monoenergetic neutrons. Calculations of Eq. (3) with $d\sigma/d\Omega$ as a variable parameter have been made to learn how sensitive the integral is to this factor. These

[16] Somewhat similar results have also been obtained by W. D. Allen, Atomic Energy Research Establishment, Harwell Report NP/R 1667, 1955 (unpublished).

[17] These measurements were made by the photographic emulsion technique. I should like to thank Dr. Rosen for permission to quote these results.

[18] E. T. Jurney and C. W. Zabel, Phys. Rev. **86**, 594 (1952); Los Alamos Scientific Laboratory Report LA-1339 (unpublished).

calculations have shown that if the radial and axial ring thicknesses are approximately the same (within a factor of 2) then σ_{in} is quite insensitive to the particular form of the angular distribution. In fact, the change in σ_{in} was generally less than 1 to 2% even when an isotropic angular distribution was assumed. Thus Eq. (3) is seen to treat correctly the inelastically scattered neutrons, which are generally assumed to have an isotropic angular distribution, providing that the attenuation coefficient μ does not change appreciably with energy. The angular distributions actually used in the calculations of cross sections were those of reference 18.

For larger rings, the ratio Y_2/Y_1 becomes large enough to indicate that it is not sufficient to consider only two interactions in the scatterer. However, if one extends the method indicated above to successive interactions, the calculations immediately become exceedingly tedious. Therefore, the assumption has been made that P_{i+1}/P_i is a constant (P_i is the probability of the ith collision), since the necessary quantities can now be obtained from Eqs. (2) and (3) with the help of the following relations:

$$\begin{aligned} Y_1&=N_0P_1(\sigma_{in}/\sigma_t),\\ Y_2&=N_0k_2P_2(\sigma_{in}/\sigma_t),\\ Y=\sum Y_i&=N_0(\sigma_{in}/\sigma_t)\sum k_iP_i \qquad (4)\\ &=N_0P_1(\sigma_{in}/\sigma_t)\sum k_ia^{i-1}, \end{aligned}$$

where $a=P_{i+1}/P_i=$constant, and N_0k_i is the number of neutrons that can produce an inelastic event at the ith interaction. This assumption has been tested for a number of different cases by calculating the probability of the first five collisions in the ring by a Monte Carlo technique. These calculations have shown that P_{i+1}/P_i is indeed approximately constant as long as the radial and axial thickness of the ring do not differ by more than a factor of two. Under these conditions the two methods of correcting for multiple scattering [Monte Carlo and Eq. (4)] give cross sections that agree within at least 1%.

In order to test the accuracy of the calculations outlined above, the cross section for excitation of the 847-kev state in Fe^{56} was measured for a number of scattering rings of different sizes. The cross sections calculated from Eq. (2) are shown in Fig. 3 plotted against ring thickness, together with the cross sections after correction for multiple scattering. The agreement of the corrected cross sections is remarkably good and indicates that the multiple-scattering problem has been treated correctly. It is significant that the multiple-scattering correction is appreciable even for the smaller rings. This indicates that it is not worth while to sacrifice gamma-ray intensity by making a sample small in an attempt to avoid the problem of multiple-scattering corrections.

Since the multiple-scattering corrections require a great deal of tedious computing unless a high-speed

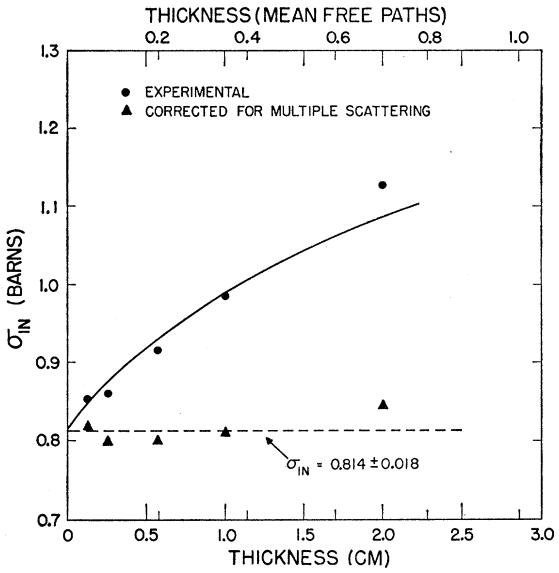

FIG. 3. Cross section for excitation of the 847-kev gamma ray in Fe by neutron inelastic scattering as measured with rings of different sizes. The inner and outer diameters were 5.08 cm and 7.08 cm, respectively, with only the axial thickness being varied. The circles give the cross sections calculated from Eq. (2), while the triangles give these cross sections after correction for multiple neutron scattering. The solid curve shows the theoretical variation of the gamma-ray yield caused by multiple scattering.

computer is available, it is interesting to consider alternative ways of calculating the inelastic scattering cross sections. The easiest is to neglect completely the effects of all neutron scattering and to assume that the neutron flux is constant throughout the scatterer, in other words that the effects of multiple scattering just cancel out the neutron attenuation at the first collision. This method has also been used to calculate the gamma-ray cross sections to be presented in Sec. IV. The root-mean-square difference between the cross sections calculated in this way and those calculated with the multiple-scattering corrections was only 3.5%, with the simple method generally giving smaller cross sections.

3. Errors

The principal errors in the measurement of the gamma-ray cross sections arise in the determination of the gamma-ray yield and the neutron flux. It has been shown that the standard error in the photopeak efficiency is about 2% in the range 0.5 to 2.8 Mev. Above and below this energy range, where calculated efficiencies were used, the photopeak efficiency is known with an accuracy of 5 to 10%. With more work it seems possible that this figure could be reduced to 5% or less. The determination of the gamma-ray yield also involves a correction for self-absorption in the scattering ring. If this correction is kept below 25%, the error it contributes to the yield is only about 1%.

The measurement of the neutron flux in the experiments described here is believed to have a standard

error of about 6%. As mentioned previously this is twice the error involved in flux measurements with a counter telescope, the increased error being due to apparent inconsistencies between the determination of the long counter efficiency with the counter telescope[15] and with calibrated Ra-Be sources.[14] From the work shown in Fig. 3 it appears that the additional error introduced in making corrections for neutron multiple scattering is less than 2%, provided the correction is of the order of 50% or less. It is necessary also to consider the possible presence of the anomalous low-energy neutrons mentioned in the preceeding section.

Since many elements can be obtained with purities of 99% or better, the error in determining the number of nuclei per cm^3 is generally negligible. In those cases where the purity is questionable, however, a chemical analysis can be made.

Since the counting rates are usually high enough to give a negligible statistical error, one sees from a consideration of the errors listed above that the standard error in these experiments could be as low as 8% whereas if a counter telescope were used for the neutron flux measurements the error would be reduced to 5%. However, in many cases the problem of determining the background to be subtracted introduces the largest source of error. Therefore, these figures apply only to strong gamma rays. Additional errors arise from the process of analyzing a complicated pulse-height spectrum to obtain the contribution of each gamma ray. These points are considered in more detail in the section on background.

IV. RESULTS

In the experiments described here, the neutrons were incident on the ring scatterers at an average angle of 5°. Since the detector was at the center of the ring, the angle of observation of the gamma rays with respect to the neutron beam was 95°. Strictly speaking then, the experiments gave the differential cross section for

TABLE I. Gamma rays from neutron inelastic scattering. In the second column the isotope emitting the gamma ray is given, where it can be identified. A comparison with the energies obtained from other reactions and from radioactive decay is given in the fourth column.

Element	Isotope	$E\gamma$ (Mev)	Comparison	Reference
Beryllium	Be^{9}	None		
Boron	Li^{7}	0.478±0.004	0.477	a
	B^{10}	0.717±0.007	0.719	b
Carbon	C^{12}	4.42 ±0.03	4.43	a
Nitrogen	N^{14}	2.30 ±0.05	2.31	a
Oxygen	O^{16}	6.094±0.06	6.14	a
Fluorine	F^{19}	0.110±0.001	0.110	a
	F^{19}	0.197±0.002	0.197	a
	F^{19}	1.234±0.020	1.233	c
	F^{19}	1.358±0.010		
	F^{19}	1.46 ±0.030	1.455	c
	F^{19}	1.56 ±0.03		
Magnesium	Mg^{24}	1.368±0.010	1.368	d
	Mg^{25}	1.616±0.016	1.612	d
	Mg^{26}	1.820±0.018	1.825	d
Aluminum	Al^{27}	0.166±0.003		
	Al^{27}	0.840±0.008	0.843	d
	Al^{27}	1.017±0.010	1.013	d
	Al^{27}	2.21 ±0.020	2.211	d
Sulfur	P^{32}	0.077±0.002	0.077	d
	S^{32}	2.23 ±0.020	2.25	d
Calcium	K^{40}	0.030±0.002	0.032	d
	Ca^{40}	0.508±0.005	0.51094	e
	K^{40}	0.767±0.007		
	K^{40}	0.877±0.017		
	Ca^{44}	1.152±0.020	1.16	d
	Ca^{40}	3.74 ±0.03	3.731	d
	Ca^{40}	3.9 ±0.1	3.900	d
Iron	Fe^{57}	0.123±0.0012	0.1228	f
	Fe^{56}	0.847±0.008	0.845	g
	Fe^{56}	1.241±0.012	1.24	g
	Fe^{54}	1.405±0.010	1.413	h
		2.18 ±0.06		
		2.3 ±0.1		
Nickel	Ni^{60}	0.827±0.008	0.85	i
	Ni^{60}	1.329±0.010	1.3325	j
	Ni^{58}	1.453±0.014	1.453	k
	Ni^{60}	2.18 ±0.04	2.158	l
Copper	Cu^{65}	0.365±0.005	0.37	m
	Cu^{63}	0.651±0.006	0.669	k
		0.764±0.010		
	Cu^{63}	0.958±0.010	0.968	k
	Cu^{65}	1.110±0.010	1.12	m
	Cu^{63}	1.325±0.010	1.326	k
	Cu^{63}	1.41 ±0.03	1.410	k
	Cu^{65}	1.47 ±0.03	1.49	m
	Cu^{63}	1.55 ±0.03	1.549	k
	Cu^{63}	1.88 ±0.04	1.89	n
		2.07 ±0.02		
	Cu^{63}	2.52 ±0.03	2.60	n
Tantalum	Ta^{181}	0.137±0.002	0.137	o
	Ta^{181}	0.164±0.004	0.166	o
	Ta^{181}	0.350±0.004	0.344	p
	Ta^{181}	0.485±0.005	0.481	p
Lead	Pb^{206}	0.533±0.005	0.5375	q
	Pb^{207}	0.570±0.010	0.569	r
	Pb^{206}	0.661±0.010		
	Pb^{206}	0.802±0.008	0.8033	q
	Pb^{207}	0.888±0.010	0.894	r
	Pb^{206}	1.43 ±0.03		
	Pb^{206}	1.73 ±0.03		
	Pb^{208}	2.620±0.020	2.61425	s
Bismuth	Bi^{209}	0.904±0.009		
	Bi^{209}	1.615±0.016		
	Bi^{209}	2.600±0.020		

[a] F. Ajzenberg and T. Lauritsen, Revs. Modern Phys. **27**, 77 (1955).
[b] Craig, Donahue, and Jones, Phys. Rev. **88**, 808 (1952).
[c] Toppel, Wilkinson, and Alburger, Phys. Rev. **101**, 1485 (1956).
[d] P. M. Endt and J. C. Kluyver, Revs. Modern Phys. **26**, 95 (1954).
[e] Muller, Hoyt, Klein, and DuMond, Phys. Rev. **88**, 775 (1952).
[f] D. E. Alburger and M. A. Grace, Proc. Phys. Soc. (London) **A67**, 280 (1954).
[g] Sakai, Dick, Anderson, and Kurbatov, Phys. Rev. **95**, 101 (1954).
[h] Phillips, Gossett, Schiffer, and Windham, Phys. Rev. **99**, 655 (1955).
[i] Nussbaum, Van Lieshout, Wapstra, Verster, Ten Haaf, Nijgh, and Orstein, Physica **20**, 555 (1954).
[j] Lindström, Hedgran, and Lind, Phys. Rev. **89**, 1303 (1953).
[k] Schiffer, Windham, Gossett, and Phillips, Phys. Rev. **99**, 655 (1955).
[l] J. L. Wolfson, Can. J. Phys. **33**, 886 (1955).
[m] K. Siegbahn and A. Ghosh, Phys. Rev. **76**, 307 (1949).
[n] Huber, Medicus, Preiswerk, and Steffen, Helv. Phys. Acta **20**, 495 (1947).
[o] T. Huus and J. H. Bjerregaard, Phys. Rev. **92**, 1579 (1953).
[p] Burson, Blair, Keller, and Wexler, Phys. Rev. **83**, 62 (1951).
[q] D. E. Alburger and M. H. L. Pryce, Phys. Rev. **95**, 1482 (1954).
[r] D. E. Alburger and A. W. Sunyar, Phys. Rev. **99**, 695 (1955).
[s] G. Lindström, Phys. Rev. **87**, 678 (1952).

gamma-ray emission at 95°; however, the results quoted later will be this differential cross section multiplied by 4π. This is the same as the total inelastic cross section if one assumes an isotropic angular distribution for the gamma rays. For excited states with a spin of 0 or 1/2 this assumption is justified; in other cases it will be necessary to measure the gamma-ray angular distribution in order to obtain the correct total inelastic cross section. It is perhaps worth noting that the proper corrections can be made if the relative angular distribution is known from 0° to 90° or 90° to 180° since the narrow width of bound states compared to their spacing guarantees angular symmetry about 90°.

Angular distributions of the stronger gamma rays can be measured by moving the gamma-ray detector along the axis of the scattering ring. This method has the disadvantage that the detection efficiency varies with angle; however, a correction for this variation can be calculated. In this way Day and Walt have obtained the angular distributions of several gamma rays, which were found to have the expected symmetry about 90°.[19]

Unless stated otherwise, the pulse-height spectra and cross sections discussed in the following sections have been obtained at a neutron energy of 2.557 Mev. However, in a few cases higher energies were used where they were necessary in order to excite the first excited state. These will be mentioned specifically.

The energies of the strong gamma rays, whose photopeak positions could be measured with good precision, have generally been assigned an accuracy of about 1%. This is based on the author's subjective feeling that the results should not often be farther from the correct value than this. In general, the reproducibility of the gamma-ray energies was within a few tenths of a percent, except for the weaker lines. From a comparison of the energies obtained here with accurate energies obtained from other experiments, it appears that the errors quoted here represent a 95% confidence limit; in other words they are approximately two standard deviations. The results of the gamma-ray energy measurements for a number of elements are summarized in Table I, together with a comparison with the best energy values obtained from other types of experiments.

The cross sections obtained as described above are given in Table II. The corrections for multiple scattering obtained from Eqs. (3) and (4) have been used. In addition, a correction has been applied to Eq. (2), to take into account the non-normal incidence of the neutrons on the scattering rings. The results contained in Tables I and II are discussed in more detail below.

1. Background

In many cases the limitation on the cross-section accuracy that is obtainable is provided by the presence of background peaks in the pulse-height distribution. These peaks are produced partly by gamma rays resulting from neutron interactions in the room in which the experiment is carried out. However, a second and

[19] R. B. Day and M. Walt (unpublished).

TABLE II. Cross sections for gamma rays from neutron inelastic scattering. The cross sections given here are 4π times the differential cross section at 95°.

Element	E_n (Mev)	$E\gamma$ (Mev)	Isotope	Cross section (millibarns)	Isotopic cross section (millibarns)
Beryllium	2.56	1.8	Be^{9}	<0.3	<0.3
	2.56	2.2	Be^{9}	<0.2	<0.2
	2.74	1.8	Be^{9}	<1.8	<1.8
	2.74	2.2	Be^{9}	<0.3	<0.3
B^{10}	2.56	0.717	B^{10}	31±3	31
Carbon	6.58	4.42	C^{12}	353±59	357
Nitrogen	3.95	2.30	N^{14}	6±3	6
Oxygen	7.06	6.094	O^{16}	104±25	104
Fluorine	2.56	0.110	F^{19}	193±38	193
	2.56	0.197	F^{19}	537±72	537
	2.56	1.234	F^{19}	50±13	50
	2.56	1.358	F^{19}	307±32	307
	2.56	1.46	F^{19}	57±16	57
	2.56	1.56	F^{19}	21±10	21
Magnesium	2.56	1.368	Mg^{24}	485±42	618
	2.56	1.616	Mg^{25}	19±4	189
	2.56	1.820	Mg^{26}	17±3	151
Aluminum	2.56	0.166	Al^{27}	1.6±0.4	1.6
	2.56	0.840	Al^{27}	64±7	64
	2.56	1.017	Al^{27}	142±13	142
	2.56	2.21	Al^{27}	87±8	87
Sulfur	2.56	0.077	S^{32}	12±2	13
	2.56	2.23	S^{32}	173±16	181
Calcium	3.95	0.030	Ca^{40}	125±63	129
	3.95	0.508	Ca^{40}	102±15	105
	3.95	0.767	Ca^{40}	71±18	73
	3.95	0.877	Ca^{40}	7±4	7
	3.95	1.152	Ca^{44}	23±6	1136
	3.95	3.74	Ca^{40}	73±30	75
	3.95	3.9	Ca^{40}	36±16	37
Iron	2.56	0.123	Fe^{57}	12±2	537
	2.56	0.847	Fe^{56}	859±69	936
	2.56	1.241	Fe^{56}	41±5	46
	2.56	1.405	Fe^{54}	47±5	798
	2.56	2.18		5±1	
	2.56	2.3		2±1	
Nickel	2.56	0.827	Ni^{60}	56±10	214
	2.56	1.329	Ni^{60}	181±21	692
	2.56	1.453	Ni^{58}	387±37	570
	2.56	2.18	Ni^{60}	17±5	65
Copper	2.56	0.365	Cu^{65}	49±10	158
	2.56	0.651	Cu^{63}	71±18	103
	2.56	0.764		47±15	
	2.56	0.958	Cu^{63}	367±48	531
	2.56	1.110	Cu^{65}	166±21	538
	2.56	1.325	Cu^{63}	110±18	160
	2.56	1.41	Cu^{63}	60±20	87
	2.56	1.47	Cu^{65}	30±15	96
	2.56	1.55	Cu^{63}	49±10	71
	2.56	1.88	Cu^{63}	26±9	38
	2.56	2.07		37±7	
	2.56	2.52	Cu^{63}	<3	<4
Tantalum	2.56	0.137	Ta^{181}	452±64	452
	2.56	0.164	Ta^{181}	244±37	244
	2.56	0.350	Ta^{181}	138±42	138
	2.56	0.485	Ta^{181}	855±110	855
Lead	2.56	0.533	Pb^{206}	143±26	584
	2.56	0.570	Pb^{207}	215±38	969
	2.56	0.661	Pb^{206}	69±21	281
	2.56	0.802	Pb^{206}	344±37	1407
	2.56	0.888	Pb^{207}	143±21	644
	2.56	1.43	Pb^{206}	32±16	129
	2.56	1.73	Pb^{206}	48±21	195
Bismuth	2.56	0.904	Bi^{209}	427±53	427
	2.56	1.615	Bi^{209}	264±26	264

more important source of background in the experiments described here arises from inelastic scattering and neutron capture in the scintillation crystal itself. The neutrons producing this background may be scattered into the crystal from the room, but the principal source is the ring scatterer itself. Figures 4 and 5 show typical pulse-height distributions obtained at neutron energies up to 3 Mev when a carbon scatterer is used. At these energies gamma rays can be produced in the carbon isotopes only by radiative capture, and it is known that the cross section for this process is very low.[20] Thus the pulse-height distributions shown here represent background effects entirely. In general, it can be seen that the shape of these background curves changes slowly with neutron energy. The fact that the higher energy lines disappear with decreasing neutron energy suggests that they arise from inelastic scattering in the crystal; however, the growth in intensity of the 138-kev gamma ray suggests that it originates in an (n,γ) reaction.

The work of Lind and Van Loef[21] on inelastic neutron scattering in I^{127} shows that the following gamma rays of those shown in Figs. 4 and 5 arise from neutron interactions with I^{127}: 58, 138, 204, 396, 441, 634, 742, and 1012 kev. Many of these also show up in the decay of Te^{127} and Xe^{127},[22] although the agreement of the energies is sometimes outside the accuracy of the experiments. More careful work on inelastic scattering in I^{127} would be required to clear up the discrepancies between the energies of some of the gamma rays observed in inelastic scattering and those observed following the decay of Te^{127} and Xe^{127}. The gamma ray

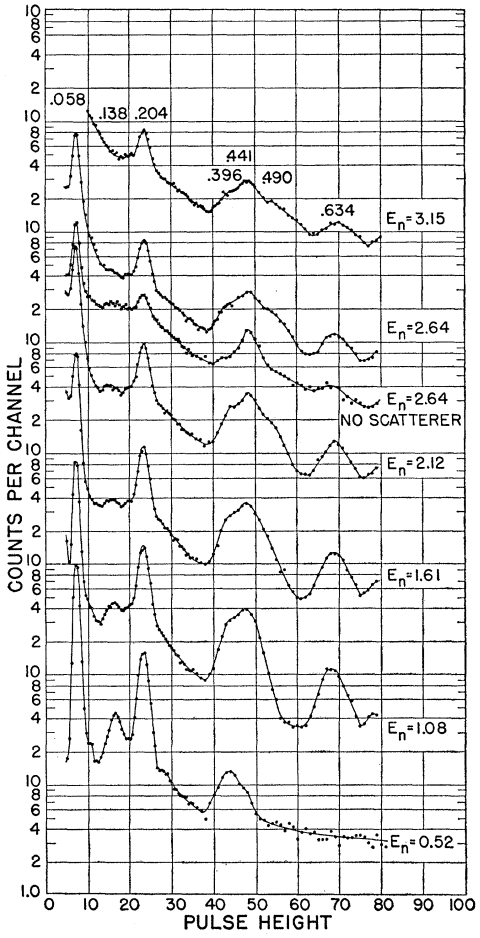

FIG. 4. Low-energy background pulse-height distribution produced by neutrons of the energies shown, normalized to a constant neutron flux incident on the scatterer. A carbon ring scatterer was used in the arrangement illustrated in Fig. 1. Photopeak energies are given in Mev just above the top curve. The ordinate changes by a factor of 10 for each energy; however, the same scale is used for the two curves at E_n=2.64 Mev.

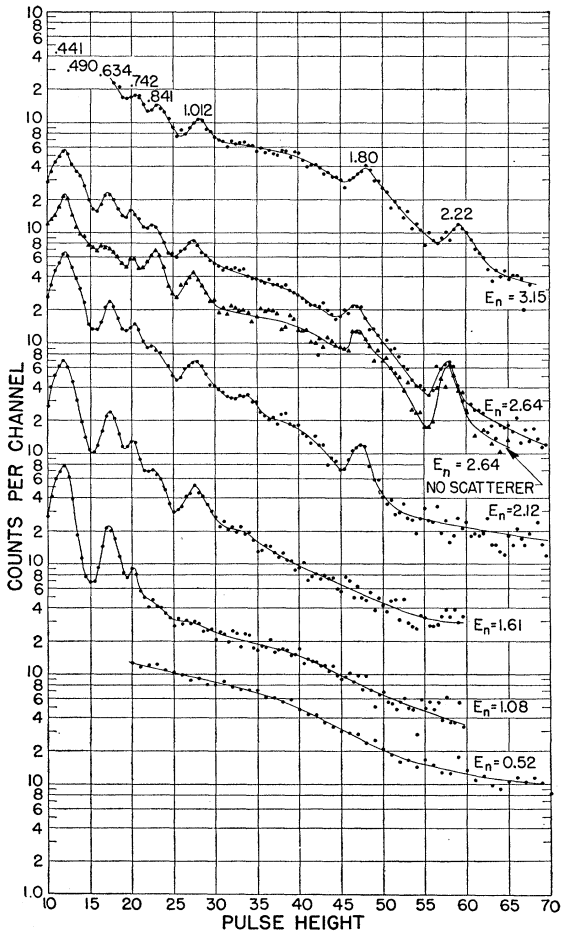

FIG. 5. Higher energy background pulse-height distribution produced by neutrons of the energies shown, normalized to a constant neutron flux incident on the scatterer. A carbon ring scatterer was used in the arrangement illustrated in Fig. 1. Photopeak energies are given in Mev just above the top curve. The ordinate changes by a factor of 10 for each energy; however, the same scale is used for the two curves at E_n=2.64 Mev.

[20] F. Ajzenberg and T. Lauritsen, Revs. Modern Phys. **27**, 77 (1955).

[21] J. J. Van Loef and D. A. Lind, Phys. Rev. **98**, 224 (1955), and J. J. Van Loef, reference 2.

[22] J. P. Mize and J. D. Knight (private communication).

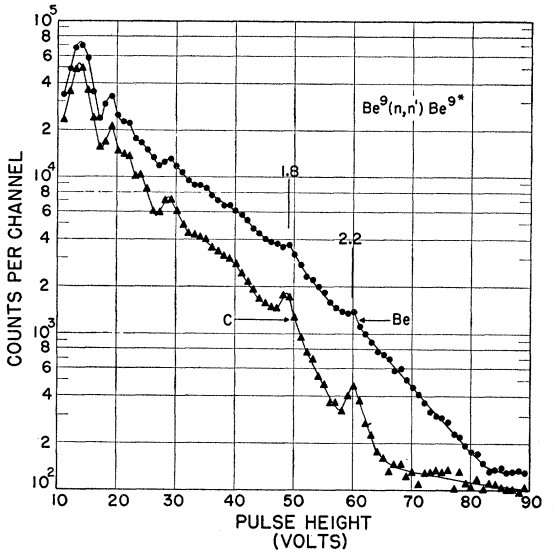

FIG. 6. Pulse-height distribution obtained with a beryllium ring, together with the background from a carbon ring. $E_n = 2.56$ Mev.

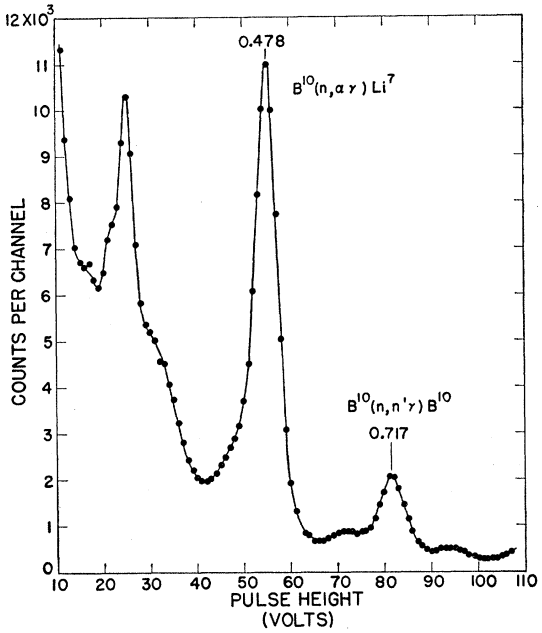

FIG. 7. Pulse-height distribution for B^{10}. $E_n = 2.56$ Mev.

at 441 kev may also be due in part to inelastic scattering in Na^{23}.

The two-inch diameter photomultiplier used for these pulse-height distributions was not completely shielded from the direct neutron beam by the tungsten cone. When smaller phototubes become available, a detector made with one of them showed no peaks at 1.8 and 2.2 Mev, and in addition the peak at 1 Mev was reduced in size. It seems probable that the 1-Mev and 2.2-Mev peaks originate in inelastic neutron scattering in the aluminum light shield, while the 1.8-Mev line comes from the silicon in the tube envelope. Studies of the background as a function of the distance of the detector from the neutron source indicate that the 841-kev gamma ray arises mainly from inelastic scattering in the iron floor of the accelerator building. A part of this line may also be contributed by inelastic scattering in aluminum.

The peaks mentioned above are superimposed on a pulse-height continuum produced by two effects: (1) inelastic scattering in I^{127} involving unresolved levels above 1 Mev, and (2) radiative capture. This continuum is generally not so objectionable as the discrete peaks since it can be subtracted from an observed pulse-height spectrum more easily.

Since the differential cross sections for neutron scattering at 95° are usually not known, it is not possible to measure the exact background in each case by observing the pulse-height distribution with a carbon ring of suitable size. In addition there is the difficulty that the spectrum of scattered neutrons would not be the same. Therefore, the procedure used in subtracting the background has been to normalize the background obtained with a carbon scatterer at the appropriate primary energy to that part of the pulse-height distribution above the energy of the highest gamma ray produced by the scatterer in question. If this procedure is not possible, one can sometimes normalize to a prominent peak that is known to be a background peak. Since the shape of the background pulse-height curve does change with energy (although slowly), this method of subtraction can introduce errors when the inelastic scattering is an appreciable fraction of the total. For the weaker gamma-ray lines in a spectrum this is often the largest source of error. In the pulse-height distributions shown later, the background has not been subtracted; thus one can see how important it is relative to the gamma rays being studied in a particular element.

After the background was subtracted, the pulse-height distribution for each gamma ray was peeled off one at a time, beginning with the highest energy line. In performing this operation, standard pulse-height distributions obtained from monoenergetic gamma rays were used. This process involved a considerable amount of trial and error in the more complicated spectra; consequently, it introduced possible additional errors in these cases.

2. Beryllium

Since Be^9 has no known levels that are stable to particle emission,[20] one would not expect to be able to observe gamma rays from neutron inelastic scattering in a beryllium target. However, it is possible that the width for decay by neutron emission might be inhibited by the centrifugal barrier or other factors to such an extent that gamma-ray decay might compete in an observable manner. This possibility is strengthened by the fact that the level at 2.4 Mev has an observed width

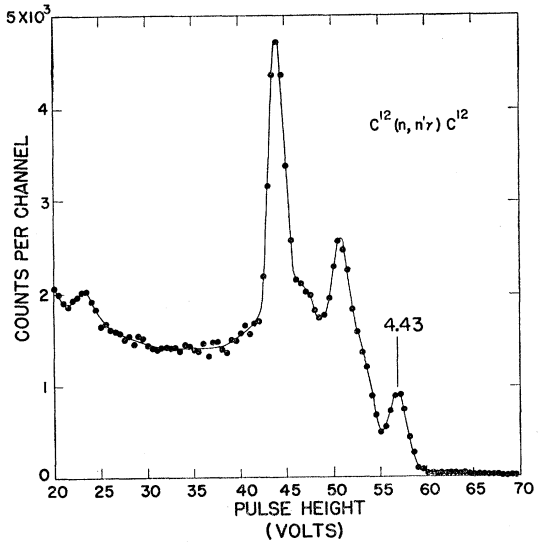

FIG. 8. Pulse-height distribution for carbon. $E_n = 6.58$ Mev.

less than 1 kev.[23] In addition, there is recent evidence for a level near 1.8 Mev,[24] and if this level has properties similar to that of the 2.4-Mev level, its lower energy for neutron emission would enhance the relative probability of gamma-ray emission.

With these considerations in mind, a search was made for gamma rays between 1.5 and 2.5 Mev that might be produced by neutron bombardment of beryllium. A typical pulse-height distribution is shown in Fig. 6, together with the pulse-height distribution obtained with a carbon scatterer. The only peaks that might be produced by gamma rays from beryllium are at 1.8 and 2.2 Mev. However, these also occur in the background, and they are almost certainly due to inelastic scattering in the Si and Al of the phototube and its light shield. An upper limit for the $Be^9(n,n'\gamma)Be^9$ reaction can be obtained by subtracting the magnitudes of the peaks in the carbon spectrum from those in the beryllium spectrum after normalizing them to the same primary neutron flux. One then obtains 0.3 and 0.2 $\times 10^{-27}$ cm^2 as the upper limits for the cross sections of the 1.8-Mev and 2.2-Mev gamma rays, respectively.

A second measurement was made at the peak of the 2.74-Mev resonance in Be, where the inelastic scattering cross section would be expected to be bigger and where the 2.4-Mev level could now be excited. Again the results were negative, the upper limits for 1.8- and 2.2-Mev gamma rays being 1.8 and 0.3×10^{-27} cm^2, respectively. The larger values for the cross sections at this energy are probably due to an increase in the background, which was measured only at 2.56 Mev.

[23] Gossett, Phillips, Schiffer, and Windham, Phys. Rev. **100** 203 (1955).

[24] F. Ajzenberg and T. Lauritsen, Revs. Modern Phys. **27**, 77 (1955); L. L. Lee, Jr., and D. R. Inglis, Phys. Rev. **99**, 96 (1955). However, the latest evidence (reference 23) shows that the experimental results do not necessarily imply the existence of a state here but can be interpreted in terms of a three-body breakup.

3. Boron-10

The scattering ring used here was made by compressing amorphous boron, enriched to 95% B^{10}, with 8% $(B^{10})_2O_3$ added as a binder. A typical pulse-height distribution is shown in Fig. 7. Only the peaks at 478 and 717 kev are definitely produced by neutron reactions in B^{10}; the others are background and Compton peaks, except for a broad peak at 23 volts that results from backscattering of the 478-kev gamma ray. If any higher energy gamma rays were present, they were concealed by background peaks and were not observable here.

It is well known that the reaction $B^{10}(n,\alpha)Li^7$ produces a 478-kev gamma ray that results from deexcitation of the first excited state of Li^7.[20] In order to show definitely that the 478-kev line observed here was from this reaction, an excitation curve as a function of primary neutron energy was measured. This curve exhibited the rapid rise at lower energies (around 500 kev) as well as the resonance at 1.9 Mev that would be expected of the $B^{10}(n,\alpha)$ reaction[25]; however, because of difficulties resulting from the presence of epithermal neutrons it was not possible to make absolute measurements of the cross section. The gamma ray at 717 kev arises from the decay of the first excited state of B^{10} after an inelastic scattering reaction. The position of this level has already been well established from a number of experiments on different reactions.[20]

4. Carbon

The first excited state of C^{12} at 4.43 Mev has been observed in many nuclear reactions. In order to see whether it could be excited by neutron inelastic scattering, a graphite ring was bombarded by 6.5-Mev neutrons. The pulse-height distribution then obtained is shown in Fig. 8. This displays the typical triad of peaks to be expected from a high-energy gamma ray. The energy of this gamma ray was obtained by comparison with the 4.43-Mev gamma ray from a Po-α-Be source and proved to be the same within the statistical accuracy. It is interesting to note that the relative background is quite low in this experiment; hence it should be easy to detect high-energy gamma rays that have much lower cross sections.

5. Nitrogen

A suitable nitrogen scattering sample was made by compressing melamine ($C_3H_6N_6$) into a disk and then machining out the center. Since no evidence of gamma rays from nitrogen was obtained at 2.56 Mev, a survey was made at primary neutron energies between 3.1 Mev and 4.2 Mev in steps of 0.1 Mev. At the higher energies there was some evidence of a 2.3-Mev gamma ray. Figure 9 shows the average of several pulse-height distributions obtained at 3.9 Mev with the melamine

[25] Petree, Johnson, and Miller, Phys. Rev. **83**, 1148 (1951).

ring and with a polyethylene ring. By measuring the pulse-height distributions alternately with the two, it was found that the peak at 30 volts was consistently broadened and shifted toward higher pulse heights for the melamine ring. From these measurements the presence of a 2.30±0.05-Mev gamma ray can be inferred. This is in good agreement with the energy of the first excited state of N^{14}.[20] Although it is energetically possible to excite a 2.14-Mev gamma ray in the $N^{14}(n,\alpha'\gamma)B^{11}$ reaction, the gamma-ray energy measurement would seem to exclude this possibility.

The reason why the inelastic scattering cross section should be so small compared with those of other light elements is not understood. Perhaps it may be due to the change of isotopic spin between the ground state and first excited state of N^{14}.

6. Oxygen

The energy level spectrum of O^{16} is quite different from that of most of the other elements in that it has no excited states below 6 Mev and the first excited state has spin zero and even parity.[20] Since 0-0 gamma-ray transitions are forbidden, this state is expected to decay primarily by the emission of nuclear pairs, and these have been observed in a number of experiments.[20] In order to determine whether this type of transition could be observed by detecting the annihilation radiation accompanying the positron decay, a hollow polyethylene toroid filled with H_2O was bombarded by 7.0-Mev neutrons. To obtain this neutron energy it was necessary to use the $H^2(d,n)He^3$ reaction, and the interaction of the bombarding deuterons with the nickel foil on the gas target cell produced such a high positron background that the pairs from the O^{16*} decay could not be detected.

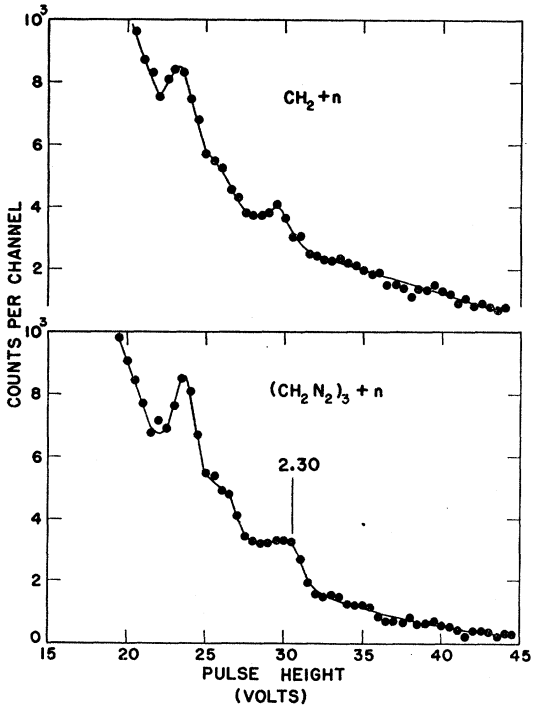

FIG. 9. Pulse-height distribution obtained with a melamine ring ($C_3H_6N_6$), together with the background from polyethylene (CH_2). E_n=3.95 Mev.

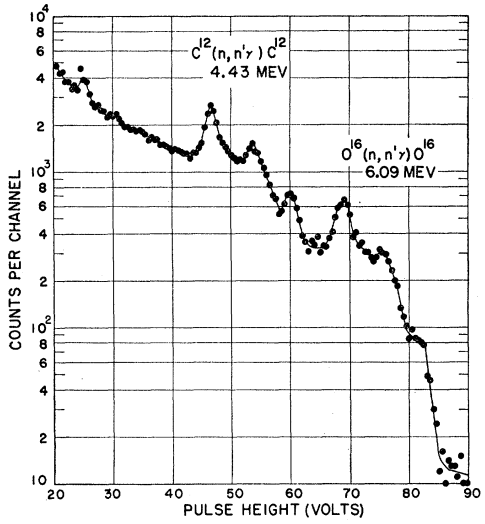

FIG. 10. Pulse-height distribution for oxygen. The three peaks between 46 and 60 volts result from inelastic scattering by the carbon in the polyethylene container. E_n=7.06 Mev.

At the neutron energy used here, it is also possible to excite the second excited state (3^-) in O^{16}. Figure 10 shows the high-energy end of the pulse-height spectrum observed. The three highest peaks are from a gamma ray whose energy is measured to be 6.09 Mev. The agreement with the energy (6.14 Mev) of the 3^- state in O^{16} is excellent and shows that this gamma ray comes from O^{16}. To show that it does not come from the carbon in the polyethylene toroid, a carbon ring was bombarded with 7-Mev neutrons. The pulse-height spectrum then exhibited only the three peaks identified in Fig. 10 as being from the reaction $C^{12}(n,n'\gamma)$.

7. Fluorine

The fluorine scattering sample was machined from Teflon (CF_2). It was immediately evident that there were two intense low-energy gamma rays, corresponding to transitions from the low-lying states originally observed by Mileikowsky and Whaling.[26] Figure 11(a) shows the low-energy spectrum, measured at a neutron energy of 1.35 Mev, where the background from neutrons and higher-energy gamma rays is smaller. The energies of the two peaks at 110 and 197 kev were measured by comparison with the gamma rays from Lu^{177}.[27] The peak at a pulse height of 39 volts is about the right energy for a gamma ray from a cascade

[26] C. Mileikowsky and W. Whaling, Phys. Rev. **88**, 1254 (1952).
[27] P. Marmier and F. Boehm, Phys. Rev. **97**, 103 (1955).

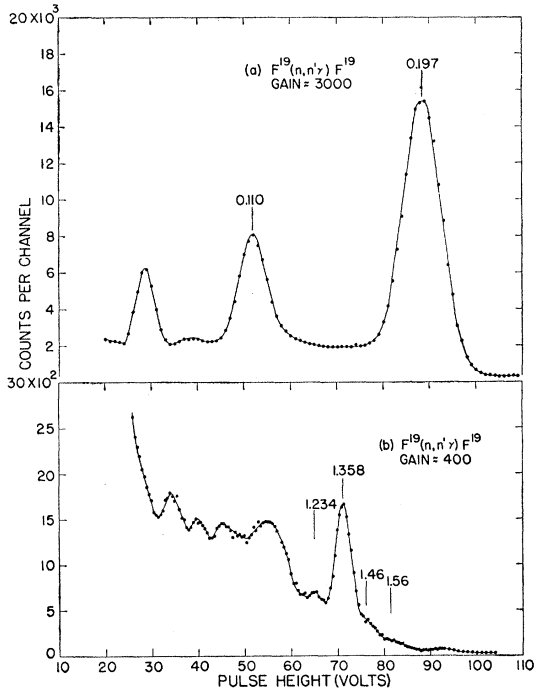

FIG. 11. Pulse-height distributions for fluorine. (a) $E_n=1.35$ Mev, (b) $E_n=2.56$ Mev.

transition between the 197- and 110-kev levels; however, it is more likely that it results from backscattering of the 110-kev gamma ray. Assuming that it is due entirely to the cascade transition, we obtain an upper limit for its probability relative to that for the 197-kev gamma ray of 6×10^{-3}.

At one time there was a suggestion from work involving the mirror nucleus, Ne^{19}, that F^{19} might have a third level near these two. Therefore, a search was made for a gamma ray between 200 and 400 kev, but without success. If such a gamma ray exists, its intensity relative to the 197-kev line is less than 1% for a primary neutron energy of 2.56 Mev, unless it lies so close to the strong 197-kev line that it cannot be resolved.

The pulse-height spectrum resulting from higher-energy gamma rays is shown in Fig. 11(b). There is good evidence here for gamma rays of 1.234, 1.358, and 1.46 Mev. The evidence for a 1.56-Mev gamma ray is somewhat weaker and depends critically on the shape of the background. Recent work[28] on proton inelastic scattering by F^{19} has shown that there are states in F^{19} at 1.342 Mev, 1.452 Mev and 1.551 Mev with the following properties: The 1.34-Mev and 1.45-Mev states decay primarily to the 110-kev state, although the latter also decays to the ground state and 197-kev state. The 1.55-Mev state decays to the 197-kev state, with an upper limit of 4% of the transitions going to the ground state. The results given here on neutron inelastic scattering by F^{19} are in good agreement with these except for the doubtful line at 1.56 Mev.

Recently Freeman[29] has published some results on the excitation curves for the 1.23-Mev and 1.36-Mev gamma rays. She finds that the thresholds for these lines in the center-of-mass system are 1.43 Mev and 1.55 Mev, respectively. Therefore, she claims that they arise from the decay of levels at 1.43 Mev and 1.55 Mev, in disagreement with the experiment of Toppel *et al.* A possible explanation is that the density of levels in the compound nucleus is not great enough to provide an observable excitation of the 1.34-Mev and 1.45-Mev levels at their true thresholds. This is strengthened by the fact that Freeman's data show a center-of-mass threshold for the 197-kev gamma ray of about 250 kev.

8. Magnesium

The principal magnesium isotope, Mg^{24}, has a well-known level at 1.370 Mev.[30] Figure 12 shows that this level is strongly excited by neutron inelastic scattering. In addition there are gamma rays present of energy 1.62 Mev and 1.81 Mev. These are very likely from Mg^{25} and Mg^{26}, respectively, since the agreement of the energies with those of known levels in these isotopes[30] is excellent. Mg^{25} is known to have lower-lying levels as well, but the high background from the Compton spectrum of the 1.37-Mev gamma ray and from neutron interactions in the crystal precluded these from being observed. A very weak line at 1.97 Mev also appeared in some of the measurements and may have been real since a level of that energy is known in Mg^{25}. However, it could not be reproduced reliably so it has not been included in these results.

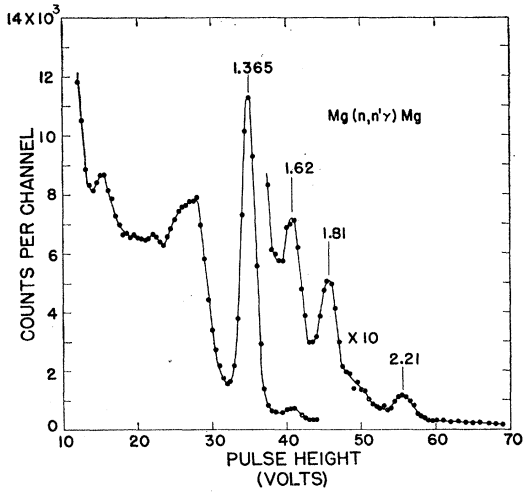

FIG. 12. Pulse-height distribution for magnesium. $E_n=2.56$ Mev.

[28] Toppel, Wilkinson, and Alburger, Phys. Rev. **101**, 1485 (1956).

[29] J. M. Freeman, Phys. Rev. **99**, 1446 (1955).

[30] P. M. Endt and J. C. Kluyver, Revs. Modern Phys. **26**, 95 (1954).

Although the 2.21-Mev gamma ray is superimposed on a background line, there is no doubt that it is really present; however, it is difficult to fit it into the level scheme of the magnesium isotopes since none of them has a known level at that energy. We have, therefore, considered the possibility that it arises from an impurity. Chemical analysis of the magnesium sample showed that although it was alleged to have a purity of >99% it actually contained 3% of aluminum. The 2.2-Mev gamma ray in aluminum appears to have a cross section large enough to account for only half of the intensity of this line in magnesium, but in view of the errors in subtracting the background it is felt that the entire effect here can probably be ascribed to the aluminum impurity.[31]

9. Aluminum

The gamma rays at 0.84 Mev, 1.02 Mev, and 2.21 Mev (shown in Fig. 13) are the ground-state transitions from the first three excited states of Al^{27}. These states are already well-known from experiments on proton inelastic scattering.[30] There has been some evidence for a level in Al^{27} near 1.7–1.8 Mev.[30,32] However, recent experiments on proton inelastic scattering[33] have failed to reveal this level, and we also find no evidence for it here.

The low-energy end of the pulse-height spectrum (not shown in Fig. 13) shows a peak at 166 kev that is well resolved from the background peak at 204 kev and that has the proper width for a 166-kev photopeak. Since its width is too small for it to be the result of backscattering of the higher energy gamma rays, it is probably a cascade gamma ray from the 1.02-Mev level to the state at 0.84 Mev. Its intensity is approximately 1% of that of the 1.02-Mev line.

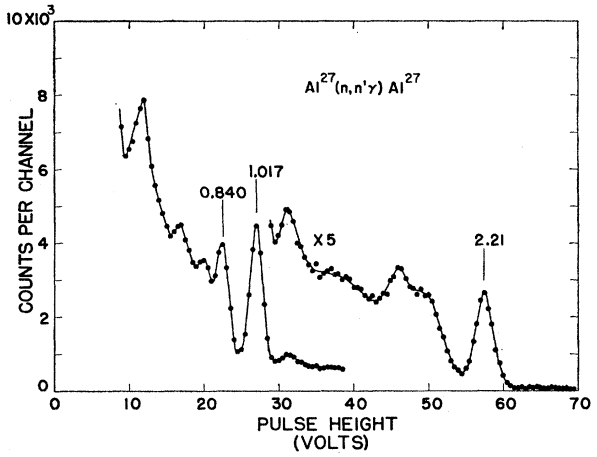

FIG. 13. Pulse-height distribution for aluminum. E_n=2.56 Mev.

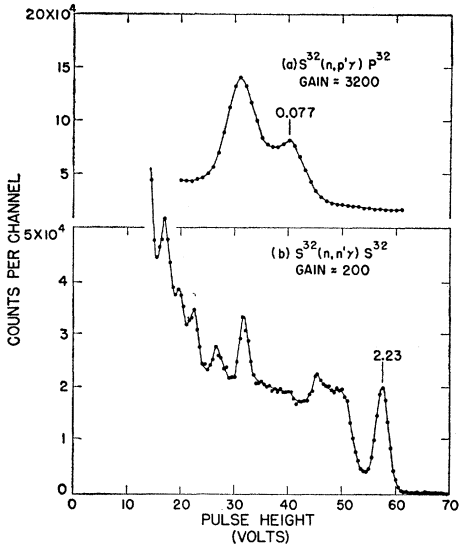

FIG. 14. Pulse-height distribution for sulfur. E_n=2.56 Mev.

According to the shell model one expects Al^{27} to have three low-lying levels of even parity and spins 1/2, 3/2, and 5/2. Since the ground state is known to be $5/2^+$,[34] one might expect the first two excited states to have spins of 1/2 and 3/2. The theoretical transition probabilities[35] then give the best agreement with the observed branching ratio if one assigns $1/2^+$ to the 0.84-Mev level and $3/2^+$ to the 1.02-Mev level.[36]

10. Sulfur

Experiments on proton inelastic scattering by S^{32} have revealed a number of levels,[30] the lowest of which is at 2.24 Mev. The pulse-height distribution [Fig. 14(b)] obtained with a sulfur ring shows a strong gamma ray at 2.23 Mev which clearly corresponds to this level. In addition, levels have also been reported at 0.5 and 1.5 Mev from the $P^{31}(d,n)S^{32}$ reaction.[37] In order to look for these levels with a smaller background, the neutron energy was reduced just below the threshold for the 2.23-Mev gamma ray. However, there was no evidence for any lower energy gamma rays that might arise from levels in S^{32}. Since the existence of levels in S^{32} below 2 Mev would contradict the known systematic behavior of first excited states in even-even nuclei,[38]

[31] I am indebted to J. J. Van Loef (Utrecht) for pointing out the difficulty in fitting this gamma ray into the magnesium level schemes and for suggesting that it arose from an aluminum impurity.

[32] Rayburn, Lafferty, and Hahn, Phys. Rev. **98**, 701 (1955).

[33] Browne, Zimmerman, and Buechner, Phys. Rev. **96**, 725 (1954).

[34] M. G. Mayer and J. H. D. Jensen, *Elementary Theory of Nuclear Shell Structure* (John Wiley and Sons, Inc., New York, 1955).

[35] J. M. Blatt and V. F. Weisskopf, *Theoretical Nuclear Physics* (John Wiley and Sons, Inc., New York, 1952).

[36] I should like to thank P. M. Endt and J. C. Kluyver (Utrecht) for calling my attention to this point.

[37] S. C. Snowdon, Phys. Rev. **87**, 1022 (1952).

[38] G. Scharff-Goldhaber, Phys. Rev. **90**, 587 (1953).

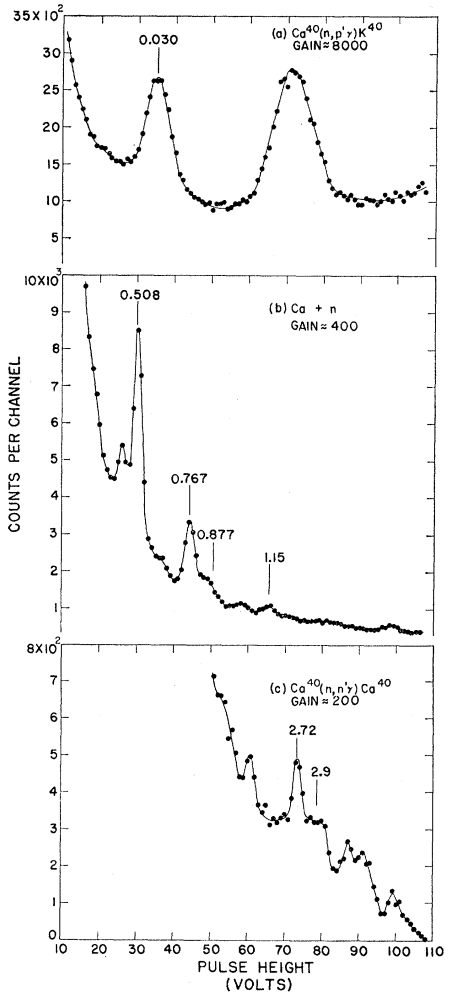

FIG. 15. Pulse-height distributions for calcium. $E_n=3.95$ Mev. The peaks identified in (c) are the pair peaks of 3.74-Mev and 3.9-Mev gamma rays.

the earlier results from the $P^{31}(d,n)S^{32}$ reaction are probably spurious. This conclusion is strengthened by a recent experiment in which no neutron groups were found from $P^{31}(d,n)$ corresponding to excited states of S^{32} below 2.2 Mev.[39]

The low-energy end of the pulse-height distribution for sulfur [Fig. 14(a)] has a peak at 77 kev that is poorly resolved from the 58-kev background peak. From the agreement of its energy with that of the first excited state[30] of P^{32} it is probable that this line originates in the $S^{32}(n,p'\gamma)P^{32}$ reaction. To test this hypothesis further, a rough excitation curve was measured for the 77-kev gamma ray. This curve was in qualitative agreement with that given in the literature[40] for $S^{32}(n,p)P^{32}$. The fact that it was not zero at a neutron energy of 2 Mev excludes the possibility that the 2.2-Mev level is a doublet with a separation of 77 kev, while the rapid decrease in cross section below 2 Mev is not what would be expected for excitation of a 77-kev level by inelastic scattering. Therefore, it is fairly certain that we have here an example of an (n,p) reaction.

11. Calcium

The principal calcium isotope is Ca^{40}, which is a doubly magic nucleus and might thus be expected to have a first excited state with spin zero and even parity.[38,41] This would then decay by nuclear pair emission as does a similar state in O^{16}. From experiments on proton inelastic scattering, the first excited state of Ca^{40} is known to be at 3.348 Mev.[30,42] In order to excite this level, a calcium ring was bombarded with 4.0-Mev neutrons. The pulse-height distributions obtained at three different amplifier gains are shown in Fig. 15. Of particular interest is the 0.508-Mev gamma ray. Within the experimental error the energy of this line is identical with that of positron annihilation radiation; however, its intensity is of the order of one hundred times too great for it to come from external pair formation by the high-energy gamma rays present. To determine whether this radiation could result from the decay of a level of Ca^{40}, a rough excitation curve was obtained. It was found that the threshold for the 0.508-Mev line occurred at a neutron energy of 3.36 $\pm$0.05 Mev in the center-of-mass system, the principal uncertainty being due to the fact that the neutron energy was varied in steps of 0.1 Mev. The excellent agreement of this threshold with the energy of the first excited state of Ca^{40} shows that this state very likely decays by emitting nuclear pairs and therefore is a 0^+ state. Nuclear pairs from this state have also been observed directly by Bonner *et al.*[43] following proton inelastic scattering.

In order to check the possibility that the annihilation radiation might result from the positron decay of a radioactive nuclide, some rough activation measurements were made. These showed that the half-life of the state giving rise to the 0.508-Mev gamma ray was less than 0.5 sec; furthermore, no positron-emitting nuclides are known that can be formed by the bombardment of calcium with 4-Mev neutrons. Thus these results strengthen the conclusion that the level at 3.35 Mev is 0^+.

The other gamma rays appearing in Fig. 15 can be assigned to known energy levels by means of the agreement of their energies with the known values. The 30-kev gamma ray probably results from the $Ca^{40}(n,p'\gamma)K^{40}$ reaction, since K^{40} has a low-lying level at 32 kev[44];

[39] F. A. El Bedewi and M. A. El Wahab, Proc. Phys. Soc. (London) **A68**, 754 (1955).
[40] E. D. Klema and A. O. Hanson, Phys. Rev. **73**, 106 (1948); T. Hürlimann and P. Huber, Helv. Phys. Acta **28**, 33 (1955).
[41] I am indebted to G. Scharff-Goldhaber for calling this to my attention and for suggesting the experiment that follows.
[42] C. M. Braams (private communication).
[43] Bent, Bonner, and McCrary, Phys. Rev. **98**, 1325 (1955).
[44] Buechner, Sperduto, Browne, and Bockelman, Phys. Rev. **91**, 1502 (1953).

furthermore, we have already seen that (n,p) reactions can be excited to an observable extent. The 0.767-Mev and 0.877-Mev gamma rays also probably result from the $Ca^{40}(n,p'\gamma)K^{40}$ reaction. Analysis of proton groups from $K^{39}(d,p)K^{40}$ has revealed the presence of levels at 0.800 Mev and 0.893 Mev,[44] and the gamma rays observed here probably represent transitions from these levels. The spin assignments suggested by Endt and Kluyver[30] (that the ground and first three excited states are 4^-, 3^-, 2^-, and 5^-, respectively) lead one to expect that the 0.80-Mev level decays to the 30-kev state and the 0.89-Mev level to the ground state. The energies of the gamma rays observed here are in agreement with this suggestion.

The 1.15-Mev gamma ray might arise from a transition between the 2.03-Mev and 0.89-Mev levels in K^{40}; however, the barrier factor for the outgoing proton in this case would probably reduce the cross section for the (n,p) reaction to such an extent that this line could not be observed. Since the agreement of its energy with that of the first excited state of Ca^{44} is excellent,[30] it is most likely that it results from inelastic scattering by this nucleus.

The high-energy part of the pulse-height spectrum in Fig. 15(c) has a group of peaks that appear to be from two closely spaced high-energy gamma rays. A peak at 2.72 Mev probably represents the pair peak of a 3.74-Mev gamma ray, while the location of the unresolved pair peak of a 3.9-Mev gamma ray is also indicated. These gamma rays are probably from the second and third excited states of Ca^{40}, which the work of Braams *et al.*[30,42] has shown to lie at 3.730 Mev and 3.900 Mev. However, it is difficult to decompose the spectrum of Fig. 15(c) into its component parts using the known line shapes of gamma rays of these energies. This difficulty may be due to the presence of additional unresolved lines. Since this spectrum has been repeated a number of times under different conditions, one can be sure that the lines indicated are really present and are not spurious; however, the values obtained for the gamma-ray cross sections are much less accurate than they would be without this uncertainty.

12. Iron

The pulse-height spectrum for iron is shown in Fig. 16. The intense line at 0.847 Mev represents a transition from the first excited state of Fe^{56}. This state is well-known from the decay of Mn^{56} [45] and Co^{56},[45,46] and has also been found in proton inelastic scattering by Fe^{56}.[47] The 1.24-Mev line occurs in the decay of Co^{56} in a transition from a state at 2.09 Mev in Fe^{56} to the first excited state.[46] From the analysis of the angular distribution of the gamma radiation from aligned Co^{56} nuclei[48] it has been shown that the 2.09-Mev level is 4^+. It is interesting to note that a spin change of 4 units is necessary to excite this level, yet it is easily observable only 500 kev about its threshold. This fact suggests that neutron inelastic scattering may prove useful in nuclear spectroscopy in investigating energy levels that cannot be reached by inelastic scattering of charged particles or by radioactive decay.

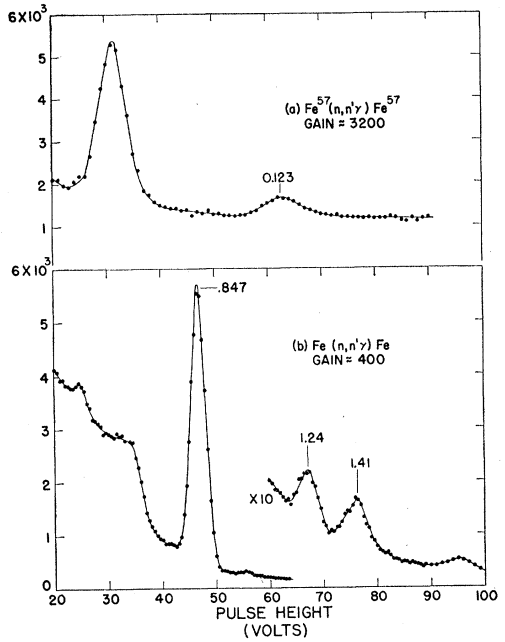

FIG. 16. Pulse-height distribution for iron. $E_n = 2.56$ Mev.

In addition, neutron inelastic scattering is useful in determining decay schemes since the primary neutron energy at which a particular gamma ray appears is often very close to the theoretical threshold for exciting the level from which the gamma ray comes. To see whether the 1.41-Mev gamma ray was a cascade line from a level at 2.26 Mev in Fe^{56} to the 0.85-Mev level, the primary neutron energy was lowered to 2.18 Mev. Since the line was still present, it was clear that it could not be in cascade with the 0.85-Mev gamma ray, and was, therefore, probably from a 1.4-Mev level in one of the iron isotopes. Since the systematics of even-even nuclei would predict a level in Fe^{54} at 1.4 Mev,[38] there was a good probability that the 1.4-Mev gamma ray arose from inelastic scattering in this isotope. This has been confirmed by recent experiments on proton and neutron inelastic scattering by Fe^{54} using separated targets.[47,49]

Fe^{57} has an excited state at 137 kev that decays

[45] Hollander, Perlman, and Seaborg, Revs. Modern Phys. **25**, 469 (1953).
[46] Sakai, Dick, Anderson, and Kurbatov, Phys. Rev. **95**, 101 (1954).
[47] Phillips, Gossett, Schiffer, and Windham, Phys. Rev. **99**, 655 (1955).
[48] Poppema, Siekman, and Van Wageningen, Physica **21**, 223 (1955).
[49] R. M. Sinclair, Phys. Rev. **99**, 1351 (1955); Beghian, Hicks, and Milman, Phil. Mag. **46**, 963 (1955).

principally to its first excited state at 14 kev.[45,50] Although this isotope has an abundance of only 2.2% in normally occurring iron, it was of interest to see whether inelastic scattering could be observed. Accordingly, an iron ring with a radial thickness of 1.5 mm was made in order to minimize the self-absorption of the low-energy gamma ray expected. The average of a number of pulse-height distributions obtained with this ring is shown in Fig. 16(a), and the expected gamma ray stands out clearly at 123 kev. The energy of this line is in good agreement with the energy measured for the same line following the decay of Co^{57}.[50]

In addition to the gamma rays shown in Fig. 16 there was also a suggestion of a gamma ray near 2.2 Mev. A close examination of this region with a small scintillation counter having no background peak at this energy revealed the existence of an asymmetric peak that appeared to result from two gamma rays of energy 2.18 Mev and 2.3 Mev. It is not clear where these gamma rays might originate.

13. Nickel

From the decay of Co^{60} it has become well established that Ni^{60} has a 2^+ level at 1.33 Mev and a 4^+ level at 2.50 Mev which decays by emitting a 1.17-Mev gamma ray to the 2^+ level.[45] The pulse-height distribution for nickel in Fig. 17 shows a strong line at 1.33 Mev that is clearly from the 2^+ state. Since the primary neutron energy was barely above the threshold for exciting the 4^+ state, one would not have expected to observe the 1.17-Mev gamma ray above the Compton background of the two strong lines.

Recent work on proton inelastic scattering using separated nickel targets has shown that the first excited state of Ni^{58} is at 1.45 Mev.[51] Thus the 1.45-Mev gamma ray observed here is undoubtedly from this level since its intensity is so great that it must come from either Ni^{58} or Ni^{60}, and it cannot be fitted into the Ni^{60} level scheme.

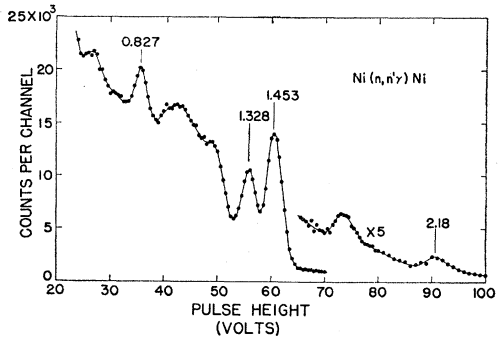

FIG. 17. Pulse-height distribution for nickel. $E_n = 2.56$ Mev.

[50] D. E. Alburger and M. A. Grace, Proc. Phys. Soc. (London) **A67**, 280 (1954).
[51] Schiffer, Windham, Gossett, and Phillips, Phys. Rev. **99**, 655 (1955).

The two other gamma rays, at 0.83 Mev and 2.18 Mev, arise from the decay of a 2.16-Mev level in Ni^{60}. The fact that the sum of the energies of the 0.83-Mev and 1.33-Mev gamma rays was the same within experimental error as the energy of the 2.18-Mev line originally suggested that the 0.83-Mev line might be a cascade transition from a 2.16-Mev level. This hypothesis was confirmed by showing that the 0.83-Mev gamma ray disappeared as the primary neutron energy was reduced to 2.18 Mev. In addition, these gamma rays have been observed by Nussbaum *et al.*[52] in the decay of Cu^{60}, and the branching ratio obtained by these investigators is in agreement with the one obtained here. A very weak 2.158-Mev gamma ray has also been observed by Wolfson[53] in the decay of Co^{60}, but the Compton background from the other gamma rays prevented his observing the 0.83-Mev line.

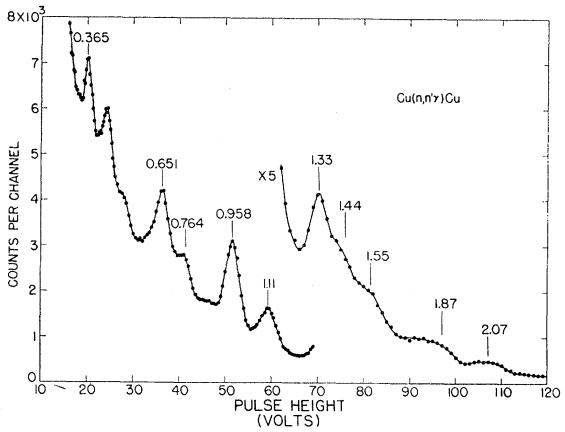

FIG. 18. Pulse-height distribution for copper. $E_n = 2.56$ Mev.

14. Copper

The pulse-height spectrum for copper, which is given in Fig. 18, was the most complicated of those observed. Because of the large number of gamma rays present the problem of decomposing the pulse-height spectrum to find the contributions of the individual lines was more difficult than usual; consequently, the errors in the intensity of the weaker gamma rays are larger than would otherwise be the case. In particular the region from 1.3 Mev to 1.6 Mev is difficult to unravel. There are clearly at least three gamma rays here, but in the analysis of some of the pulse-height spectra the 1.44-Mev line appeared to be a doublet composed of two gamma rays of energy 1.41 Mev and 1.47 Mev. Since other considerations make it plausible that both these lines should be present, they have been included in Tables I and II. However, without this additional evidence we should have been inclined to

[52] Nussbaum, Van Lieshout, Wapstra, Verster, Ten Haaf, Nijgh, and Ornstein, Physica **20**, 555 (1954).
[53] J. L. Wolfson, Can. J. Phys. **33**, 886 (1955).

say that the 1.44-Mev peak resulted from a single gamma ray.

The problem of assigning the gamma rays observed here to various levels of the copper isotopes has been greatly aided by recent measurements of proton inelastic scattering made with separated targets of Cu^{63} and Cu^{65}.[51] These measurements showed that there were levels in Cu^{63} at 0.669 Mev, 0.968 Mev, 1.326 Mev, 1.410 Mev, and 1.549 Mev, while no levels were observed in Cu^{65}. Except for the lowest energy gamma ray, these energies are in good agreement with those of the corresponding gamma rays observed here; hence the latter can be assigned to Cu^{63}. In addition, the decay of Zn^{63} has shown that there are levels in Cu^{63} at 1.89 Mev and 2.60 Mev,[45] which accounts for two of the higher-energy lines. Finally, it is possible that the 0.764-Mev line is a cascade gamma ray between the 1.41-Mev and 0.67-Mev levels. A measurement of the threshold for this gamma ray would help in settling this point, but this has not yet been done.

Although Schiffer *et al.*[51] found no excited states in Cu^{65}, it is known from the decay of Zn^{65} and Ni^{65} that there are levels at 1.11 Mev and 1.49 Mev.[45] A fairly strong 1.11-Mev gamma ray can be seen in Fig. 18, in addition to a 0.365-Mev gamma ray that is probably a transition from the 1.49-Mev level to the 1.11-Mev state. The existence of the low-energy line implies that there should also be a 1.49-Mev line since the decay of Ni^{65} shows us that the 1.49-Mev level decays also to the ground state.[45] It is because of this evidence for the excitation of the 1.49-Mev level in addition to the evidence from proton inelastic scattering for a 1.41-Mev level in Cu^{63} that we are inclined to attach somewhat more weight to the previously mentioned possibility that the 1.44-Mev gamma ray is a doublet.

The origin of the 2.07-Mev gamma ray is still unknown. It probably comes from a previously undiscovered level of this energy in one of the two copper isotopes.

15. Tantalum

The low-lying levels of Ta^{181} have recently been investigated rather extensively by means of Coulomb excitation.[54] The results have shown that there are two levels at 137 kev and 303 kev that are part of the ground-state rotational band. In order to investigate these levels by neutron inelastic scattering it was necessary to use a tantalum ring only 0.25 mm thick radially in order to reduce self-absorption of the gamma rays. The pulse-height distribution obtained with such a ring is shown in Fig. 19. Here the 137-kev gamma ray from the first excited state is strongly excited, as well as the 164-kev cascade transition from the second excited state. Although the latter gamma ray appears here only as a bump on the high-energy side of the 137-kev peak, it was easily seen in pulse-height distributions made at higher amplifier gains.

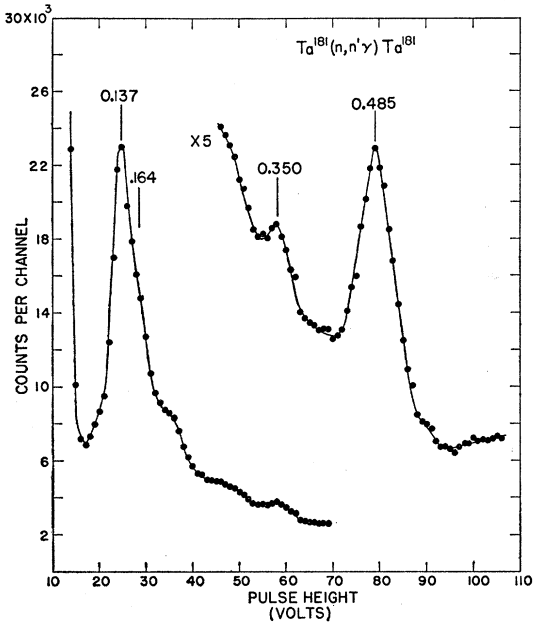

FIG. 19. Pulse-height distribution for tantalum. $E_n = 2.56$ Mev.

The 485-kev gamma ray is the ground-state transition from a level of that energy which also decays to the 137-kev level by the emission of the 350-kev gamma ray. Both of these gamma rays have been studied previously in the decay of Hf^{181}.[45]

After subtraction of the background, there was a small peak near 300 kev superimposed on the Compton peak of the 485-kev gamma ray. However, this peak was somewhat too broad for a photopeak; furthermore, the Compton distribution of the 485-kev line did not have the correct shape. The anomalous shape of the Compton distribution resulted from uncertainties in determining the correct background to be subtracted. Therefore, it was not possible to extract any quantitative information on the intensity of the line (or lines) near 300 kev. Nevertheless, it is worth noting that the 303-kev level is known to decay also to the ground state[54]; hence, the presence of the 164-kev gamma ray implies that a 303-kev gamma ray should also be present.

16. Lead

The pulse-height distribution for a lead ring is shown in Fig. 20. Since the lowest level of Pb^{208} is at 2.62 Mev,[45] it would not have been excited at a primary neutron energy of 2.56 Mev; therefore, the gamma rays seen here are all from Pb^{206} and Pb^{207} (Pb^{204} has too small an abundance for its gamma rays to be detected). However, when the primary neutron energy was increased to 3 Mev, the well-known 2.62-Mev gamma ray from Pb^{208} did appear.

[54] T. Huus and C. Zupancic, Kgl. Danske Videnskab Selskab Mat-fys. Medd **28**, No. 1 (1953); McClelland, Mark, and Goodman, Phys. Rev. **97**, 1191 (1955); N. P. Heydenburg and G. M. Temmer, Phys. Rev. **100**, 150 (1955); P. H. Stelson and F. K. McGowan, Phys. Rev. **99**, 112, 127 (1955).

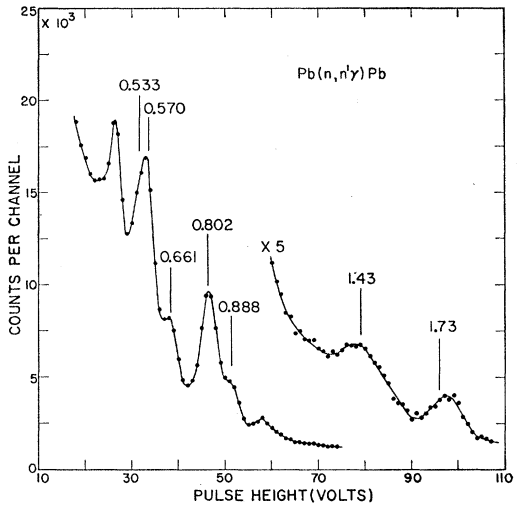

FIG. 20. Pulse-height distribution for normal lead. $E_n=2.56$ Mev.

In attempting to determine which gamma rays in Fig. 20 are to be assigned to Pb^{206} and which to Pb^{207}, the level schemes for these isotopes that have been worked out from studies of the decay of Bi^{206} [55] and Bi^{207} [56] are very useful. However, all of the low states of the lead isotopes may not be populated by the β decay of Bi^{206} and Bi^{207}; in fact, three of the gamma rays observed here do not fit into the known level schemes. Therefore, it was of considerable value in settling the origin of these lines that radiolead, which contains about 89% Pb^{206}, was available in sufficient quantities for a scattering sample to be made.[57] Figure 21 shows the pulse-height distribution obtained with such a ring after the natural background from the ring had been subtracted. Background from RaE β particles was eliminated by surrounding the NaI counter with 1.5 mm of aluminum. However, the bremsstrahlung produced by these β particles was the main source of background and could not be eliminated.

From a comparison of Figs. 20 and 21 one can see that the 0.661-Mev, 0.802-Mev, 1.43-Mev, and 1.73-Mev gamma rays are from Pb^{206} (the 1.73-Mev peak in Fig. 20 appears displaced because of the 1.8-Mev background peak). In addition the question as to the interpretation of the broad peak at 0.56-Mev in the spectrum for normal lead can now be cleared up. From Fig. 21 we see that Pb^{206} has a 0.533-Mev gamma ray, and if a photopeak of the proper width and amplitude is subtracted from Fig. 20 one is left with a 0.57-Mev peak. This is just the energy of the first excited state of Pb^{207}.[56] In addition, the 0.888-Mev gamma ray agrees well in energy with the second excited state of Pb^{207}. There is also an isomeric state in Pb^{207} at 1.63 Mev, which decays by emitting a 1.06-Mev gamma ray to the first excited state. The neutron excitation of this level has previously been measured by an activation technique[58]; however, the photopeak for the 1.06-Mev gamma ray would fall close to a background peak here, and the cross section reported for excitation of this isomeric level is then too low for it to have been detected in this experiment. Possible low-energy gamma rays were not looked for in lead because of the large self-absorption at these energies.

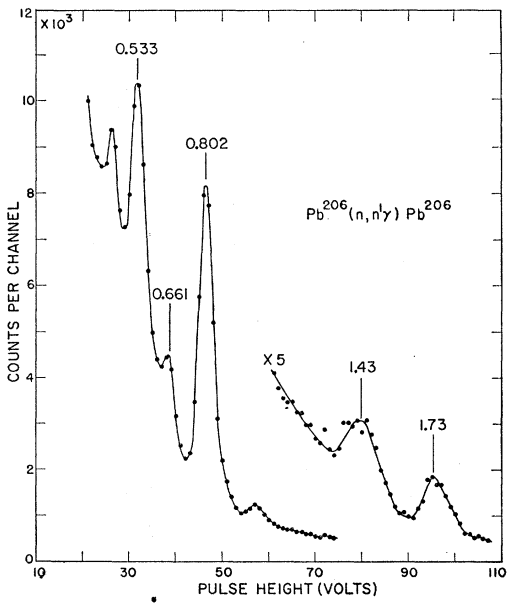

FIG. 21. Pulse-height distribution for radiolead (0.06% Pb^{204}, 89.34% Pb^{206}, 8.25% Pb^{207}, 2.35% Pb^{208}). $E_n=2.56$ Mev.

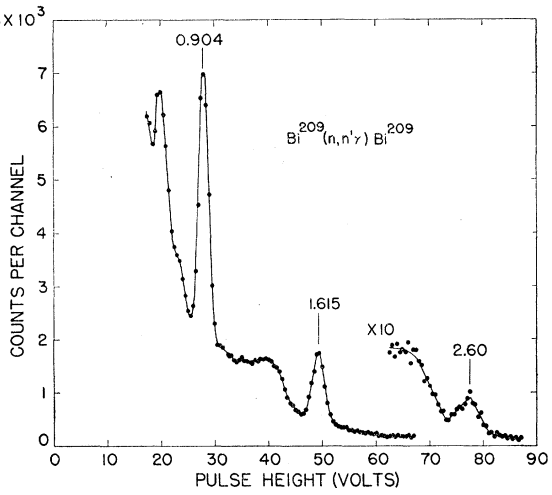

FIG. 22. Pulse-height distribution for bismuth. $E_n=2.64$ Mev.

[55] D. E. Alburger and M. H. L. Pryce, Phys. Rev. **95**, 1482 (1954).
[56] N. H. Lazar and E. D. Klema, Phys. Rev. **98**, 710 (1955); D. E. Alburger and A. W. Sunyar, Phys. Rev. **99**, 695 (1955).
[57] This material was obtained from Atomic Energy of Canada Limited, Commercial Products Division, Ottawa, Canada.
[58] P. H. Stelson and E. C. Campbell, Phys. Rev. **97**, 1222 (1955).

The 0.802-Mev and 0.533-Mev lines can be assigned to levels in Pb^{206} that are known from studies of the decay of Bi^{206}.[55] Thus the first is a transition from the first excited state, while the second is a cascade transition from a 3^+ level at 1.34 Mev to the first excited state. The other three Pb^{206} lines, however, cannot be fitted into the level scheme deduced by Alburger and Pryce.[55] This fact is not surprising when one considers that the levels above 0.80 Mev that are populated in the Bi^{206} decay all have spins greater than 2. Thus states with spins of 2 or less, which would be most easily excited in neutron inelastic scattering, would have been skipped. In order to introduce as few new levels as possible to fit these data, one might assume a level at 1.73 Mev that decays to the ground state and a level at 1.46 Mev that decays both to the ground state and to the first excited state. Recent data on the excitation curves for these gamma rays tend to support these assignments.[59]

17. Bismuth

Inelastic scattering by bismuth is of particular interest since it has not previously been possible to obtain information on the energy levels of Bi^{209} from other reactions or from radioactive decay. The pulse-height spectrum obtained with a bismuth ring is shown in Fig. 21. The three gamma rays seen here arise from ground-state transitions from excited states of the same energy. This fact has been established by the work of Kiehn and Goodman,[60] which showed that the two lower energy gamma rays had the thresholds to be expected of ground-state transitions, and by measurements here which showed that the threshold of the high-energy line was at 2.60 Mev (see Fig. 22).

[59] R. B. Day, A. E. Johnsrud and D. A. Lind, Bull. Am. Phys. Soc. Ser. II, Vol. 1, No. 1, 56 (1956).
[60] R. M. Kiehn and C. Goodman, Phys. Rev. **95**, 989 (1954).

V. ACKNOWLEDGMENTS

I should like to express my thanks to the many people whose capable assistance has contributed so much to this work. The coding of Eqs. (1) and (3) for numerical integration on the digital computers was carried out by R. B. Lazarus, who also checked all the formulas. He was assisted in the later stages of coding by J. M. Kister. The Monte Carlo theory of multiple scattering was developed by H. Kahn and the numerical calculations of this were performed under his supervision. M. Goldstein supervised the various calculations on Compton scattering cross sections that were necessary in order to evaluate the gamma-ray self-absorption in the scattering rings.

The accuracy attained in the determination of the photopeak efficiency of the NaI counter would not have been possible without the careful work of D. R. F. Cochran, who prepared the sources used in the β-γ coincidence counting and in the photopeak efficiency determinations. Much of the work in developing the β-γ coincidence technique was done by E. F. Bennett, who also made a thorough investigation of the sources of error that could arise.

The special problems that arose in the fabrication of the boron-10, nitrogen, sulfur, and calcium scattering rings were handled by J. R. Armstrong, P. F. Hartshorne, D. H. Schell, and H. Sheinberg. The mass analysis of the normal lead and radiolead was made by J. E. Hand. A number of people have assisted in operating the electrostatic generator and taking data. In particular I am indebted to R. A. Nobles, R. K. Smith, M. Walt, and D. Douglass for this. Discussions with M. Deutsch and G. Scharff-Goldhaber have been helpful in determining the levels from which some of the gamma rays originated. I have also benefited from discussions with J. R. Beyster and L. Cranberg on neutron inelastic scattering. Finally I should like to thank J. L. McKibben for his interest and support of this work.